2018

Estrogens promote misfolded proinsulin degradation to protect insulin production and delay diabetes

Beibei Xu
Tulane University

Camille Allard
Tulane University

Ana I. Alvarez-Mercado
Tulane University

Taylor Fuselier
Tulane University

Jun Ho Kim
Andong National University

See next page for additional authors

Article

Cell Reports

Estrogens Promote Misfolded Proinsulin Degradation to Protect Insulin Production and Delay Diabetes

Graphical Abstract

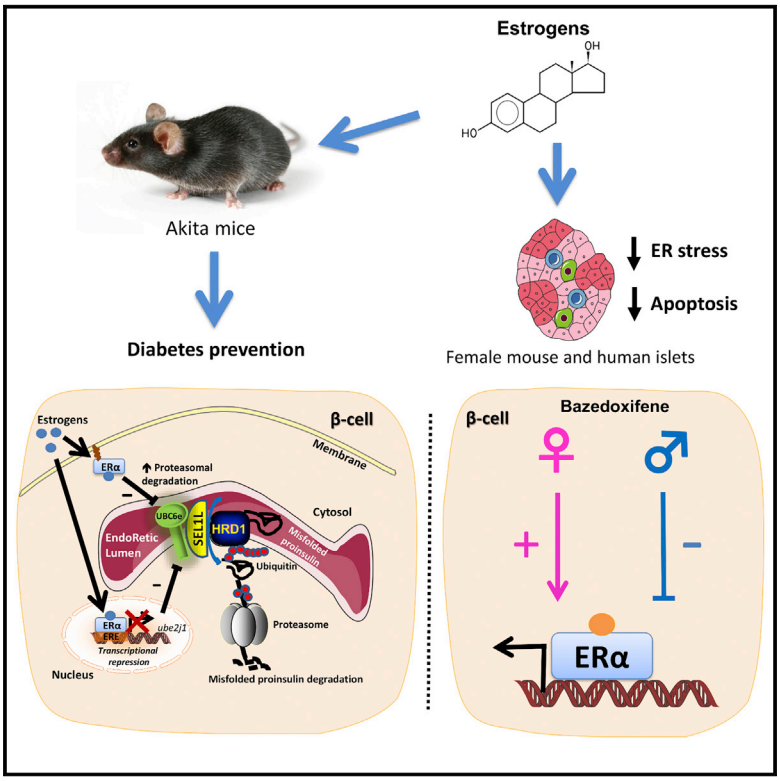

Authors

Beibei Xu, Camille Allard, Ana I. Alvarez-Mercado, ..., Peter Arvan, Z. Elizabeth Floyd, Franck Mauvais-Jarvis

Correspondence

fmauvais@tulane.edu

In Brief

Estrogens prevent diabetes in women, but the mechanism is poorly understood. Xu et al. report that estrogens activate the endoplasmic-reticulum-associated protein degradation pathway, which promotes misfolded proinsulin degradation, suppresses endoplasmic reticulum stress, and protects insulin secretion in mice and in human pancreatic β cells.

Highlights

- Estrogens prevent β cell failure and diabetes in male and in female Akita mice
- Estrogens promote misfolded Akita proinsulin proteasomal degradation in β cells
- Estrogens stabilize endoplasmic reticulum-associated protein degradation (ERAD)
- The estrogen receptor-α suppresses expression of the ERAD degrader, UBC6e

Xu et al., 2018, Cell Reports *24*, 181–196
July 3, 2018
https://doi.org/10.1016/j.celrep.2018.06.019

Cell Reports
Article

Estrogens Promote Misfolded Proinsulin Degradation to Protect Insulin Production and Delay Diabetes

Beibei Xu,[1] Camille Allard,[1] Ana I. Alvarez-Mercado,[1] Taylor Fuselier,[1,2] Jun Ho Kim,[3] Laurel A. Coons,[4,5] Sylvia C. Hewitt,[4] Fumihiko Urano,[6] Kenneth S. Korach,[4] Ellis R. Levin,[7,8] Peter Arvan,[9] Z. Elizabeth Floyd,[10] and Franck Mauvais-Jarvis[1,2,11,*]

[1]Diabetes Discovery Research and Gender Medicine Laboratory, Department of Medicine, Section of Endocrinology and Metabolism, School of Medicine, Tulane University Health Sciences Center, New Orleans, LA 70112, USA
[2]Southeast Louisiana Veterans Healthcare System Medical Center, New Orleans, LA 70112, USA
[3]Department of Food Science and Biotechnology, Andong National University, Andong, Gyeongsangbuk-do 36729, South Korea
[4]Receptor Biology Section, Reproductive and Developmental Biology Laboratory, National Institute of Environmental Health Sciences, NIH, Research Triangle Park, Durham, NC 27709, USA
[5]Department of Pharmacology and Cancer Biology, Duke University School of Medicine, Durham, NC 27710, USA
[6]Department of Medicine, Division of Endocrinology, Metabolism, and Lipid Research, Washington University School of Medicine, St. Louis, MO 63110, USA
[7]Division of Endocrinology, Veterans Affairs Medical Center, Long Beach, CA 90822, USA
[8]Departments of Medicine and Biochemistry, University of California, Irvine, Irvine, CA 92717, USA
[9]Division of Metabolism, Endocrinology and Diabetes, University of Michigan Medical School, Ann Arbor, MI 48105, USA
[10]Ubiquitin Lab, Pennington Biomedical Research Center, Louisiana State University System, Baton Rouge, LA 70803, USA
[11]Lead Contact
*Correspondence: fmauvais@tulane.edu
https://doi.org/10.1016/j.celrep.2018.06.019

SUMMARY

Conjugated estrogens (CE) delay the onset of type 2 diabetes (T2D) in postmenopausal women, but the mechanism is unclear. In T2D, the endoplasmic reticulum (ER) fails to promote proinsulin folding and, in failing to do so, promotes ER stress and β cell dysfunction. We show that CE prevent insulin-deficient diabetes in male and in female Akita mice using a model of misfolded proinsulin. CE stabilize the ER-associated protein degradation (ERAD) system and promote misfolded proinsulin proteasomal degradation. This involves activation of nuclear and membrane estrogen receptor-α (ERα), promoting transcriptional repression and proteasomal degradation of the ubiquitin-conjugating enzyme and ERAD degrader, UBC6e. The selective ERα modulator bazedoxifene mimics CE protection of β cells in females but not in males.

INTRODUCTION

Type 2 diabetes (T2D) is increasingly considered a protein misfolding disorder (Wang and Kaufman, 2016). Early in the disease, as insulin-producing pancreatic β cells increase proinsulin synthesis to adapt to nutrient overload and insulin resistance, the proinsulin load overwhelms the capacity of the endoplasmic reticulum (ER) for proper proinsulin folding and trafficking (Back and Kaufman, 2012; Eizirik and Cnop, 2010; Papa, 2012). Chronic exposure of β cells to glucose, lipids, and cytokines further compromises the ability of the ER to promote folding of proinsulin. The resultant ER stress triggers an unfolded protein response (UPR) to enhance proinsulin folding/trafficking, remove misfolded proinsulin, and restore protein homeostasis. If protein misfolding is not resolved, β cells ultimately die. The causality between proinsulin misfolding and β cell failure is best exemplified by insulin gene mutation syndromes in which mutant and misfolded proinsulin triggers irreparable UPR, leading to early insulin-deficient diabetes in humans and in the Akita mouse (Liu et al., 2010).

The female hormone 17β-estradiol (E_2) protects rodent β cells *in vivo* against multiple proapoptotic insults (Kilic et al., 2014; Le May et al., 2006; Liu et al., 2009, 2013; Liu and Mauvais-Jarvis, 2009; Tiano et al., 2011; Tiano and Mauvais-Jarvis, 2012; Wong et al., 2010), and this protection is conserved in human islets (Kilic et al., 2014; Liu et al., 2009, 2013; Liu and Mauvais-Jarvis, 2009; Tiano et al., 2011; Tiano and Mauvais-Jarvis, 2012; Wong et al., 2010). That E_2 action in β cells prevents apoptosis induced by excess lipids and glucose, oxidative stress, and proinflammatory cytokines—all conditions producing ER stress and activating the UPR (Wang and Kaufman, 2016)—led us to envision a unifying mechanism in which activation of estrogen receptors (ERs) in β cells mitigates ER stress and helps resolve the UPR. Notably, large randomized-controlled trials have shown that menopausal hormone therapy (MHT) with conjugated estrogens (CE) reduces the incidence of T2D in women (Espeland et al., 1998; Kanaya et al., 2003; Manson et al., 2013; Manson and Kaunitz, 2016; Margolis et al., 2004; Salpeter et al., 2006). The exact mechanism of this anti-diabetic effect is poorly understood and is not explained by a decrease in adiposity or insulin resistance (Mauvais-Jarvis et al., 2017b; Santen et al., 2010). In fact, CE therapy seems to protect β cell function in postmenopausal women (Mauvais-Jarvis et al., 2017b). Age-associated failure of protein folding (which is accelerated by menopause)

(Zhou et al., 2016) allows misfolded proteins to accumulate, leading to the β cell dysfunction and vulnerability associated with aging (Taylor, 2016). Therefore, in postmenopausal women, CE treatment may mitigate age-associated ER stress in β cells to protect insulin secretion and delay diabetes. To explore this hypothesis, we used mice and cells heterozygous for the Akita spontaneous mutation ($Ins2^{+/Akita}$) as a model of extreme insulin misfolding. We tested the effect of CE alone or in combination with the selective estrogen receptor modulator (SERM) bazedoxifene (BZA), a novel menopausal treatment that provides the benefits of CE, while simultaneously protecting uterine and breast tissues from estrogenic stimulation (Kharode et al., 2008; Komm, 2008, 2011; Lindsay et al., 2009).

RESULTS

CE and BZA Differentially Protect Islets and Prevent Diabetes in Male and in Female Akita Mice

We studied male Akita mice at 5 weeks of age, when they were already hyperglycemic. Treatment with CE decreased random-fed blood glucose to normoglycemic levels compared to vehicle, but BZA did not (Figure 1A). Further, BZA seemed to impair the ability of CE in preventing hyperglycemia, as the combination CE+BZA was not as efficient as CE alone in preventing hyperglycemia (Figure 1A). The blood insulin/glucose (I/G) ratio, an index of β cell function, was higher in CE- and CE+BZA-treated male mice compared to the vehicle- and BZA-treated groups (Figure 1B), indicating that CE and, to a lesser extent, CE+BZA, but not BZA alone, helped preserve insulin secretion in these mice. Fasting hyperglycemia was significantly decreased in CE-treated mice only (Figure S1A). Following an intraperitoneal glucose tolerance test (IP-GTT), CE-treated male Akita mice displayed better glucose tolerance compared to their littermates treated with vehicle, BZA, or the combination CE+BZA (Figure 1C). Accordingly, CE-treated male Akita mice exhibited higher plasma I/G index of β cell function at 30 min into the GTT compared to other groups (Figure 1D). The endogenous hormone E_2 exhibited the same anti-diabetic effect as CE in adult male Akita mice (Figures S1B and S1C). To determine whether the combination of CE with BZA protects insulin secretion and prevents diabetes when administered prior to the development of hyperglycemia, we studied normoglycemic, prepubertal 3-week-old male Akita mice. In these young mice, treatment with CE+BZA prevented the onset of hyperglycemia (Figure 1E) and was associated with a higher I/G index of β cell function compared to vehicle (Figure 1F).

Female Akita mice are not as hyperglycemic as males and are therefore rarely used in studies. Indeed, female Akita mice exhibited mild hyperglycemia at 3 weeks of age compared to male littermates (cf. Figures 1G and 1E). Given the observed protective effect of CE and E_2 in Akita males, we ovariectomized (OVX) the Akita females to test for the protective effect of endogenous E_2. When ovariectomized before puberty, vehicle-treated OVX female Akita mice developed more severe hyperglycemia compared to control sham-operated Akita littermates, suggesting that they were protected by ovarian E_2 (Figure 1G). Treatment with CE, BZA, or CE+BZA reduced the severity of hyperglycemia in OVX Akita mice compared with vehicle-treated OVX Akita mice (Figure 1G). Importantly, unlike in males, in OVX Akita mice, BZA alone prevented hyperglycemia to an extent similar to CE (Figure 1G). Accordingly, the I/G index of β cell function was improved by treatment of OVX Akita mice with CE, BZA, and CE+BZA compared to those treated with vehicle (Figure 1H). To validate that the combination of CE with BZA could also prevent diabetes in female Akita mice after sexual maturation, we treated female Akita mice with OVX after puberty, followed by treatment with CE+BZA. At 75 days of age, intact female Akita mice were mildly hyperglycemic compared to littermate males of the same age (cf. Figures 1A and 1I), suggesting that female Akita mice are protected from diabetes by endogenous E_2. Vehicle-treated OVX mature Akita mice developed hyperglycemia at levels similar to those observed in males (Figure 1i). In contrast, treatment with CE+BZA totally prevented OVX mature Akita mice from developing hyperglycemia (Figure 1i). Therefore, in young and in mature female Akita mice, CE and BZA similarly prevent the development of insulin-deficient diabetes. These results demonstrate that CE prevent β cell failure and the development of insulin-deficient diabetes in male and OVX female Akita mice. However, BZA alone prevents β cell failure and the development of diabetes in females, but not in males.

Consistent with the effect of estrogens on blood glucose described above, treatment of OVX female Akita mice with CE, BZA, and CE+BZA preserved β cell mass compared to vehicle (Figure 2A). In OVX mice, treatments with CE, BZA, or CE+BZA decreased β cell apoptosis (Figure 2B) without affecting β cell proliferation (data not shown). Furthermore, β cells of vehicle-treated mature OVX female Akita mice exhibited dilated ER and enlarged mitochondria compared to wild-type (WT) and ovary-intact Akita female mice, suggesting that endogenous E_2 prevents ER stress and mitochondrial damage in Akita β cells (Figures 2C–2E). Consistent with the protection of β cell function described earlier (Figure 1H), treatment of OVX Akita mice with CE+BZA helped retain the normal morphology of β cell ER and mitochondria (Figures 2C–2E). In adult male Akita mice, treatment with CE, and to a lesser extent CE+BZA, also helped retain higher β cell mass (Figure 2F) and pancreas insulin content (Figure 2G) compared to vehicle-treated mice, while BZA alone had no effect on these parameters (Figures 2F and 2G). The endogenous hormone E_2 exhibited the same protective effect as CE on β cell apoptosis and pancreas insulin content in male Akita mice (Figures S2A and S2B). Accordingly, CE or CE+BZA, but not BZA alone, decreased β cell apoptosis (Figure 2H) with no effect on β cell proliferation (Figure S2C). In prepubertal 3-week-old male Akita mice, consistent with the protection of β cell function and hyperglycemia described earlier (Figure 1F), treatment with the combination CE+BZA prevented the ER stress and swelling of mitochondria (Figures 2I–2K).

Together, these results demonstrate that CE and BZA prevent ER stress, mitochondrial structural alterations, and β cell apoptosis and help retain β cell mass and insulin secretion in OVX female Akita mice.

CE and BZA Differentially Prevent ER Stress in Male $Ins2^{+/Akita}$ Cells and in Female Akita Islet Cells

Because islets from male Akita mice, but not females, are destroyed early, we studied β cell protection from ER stress in

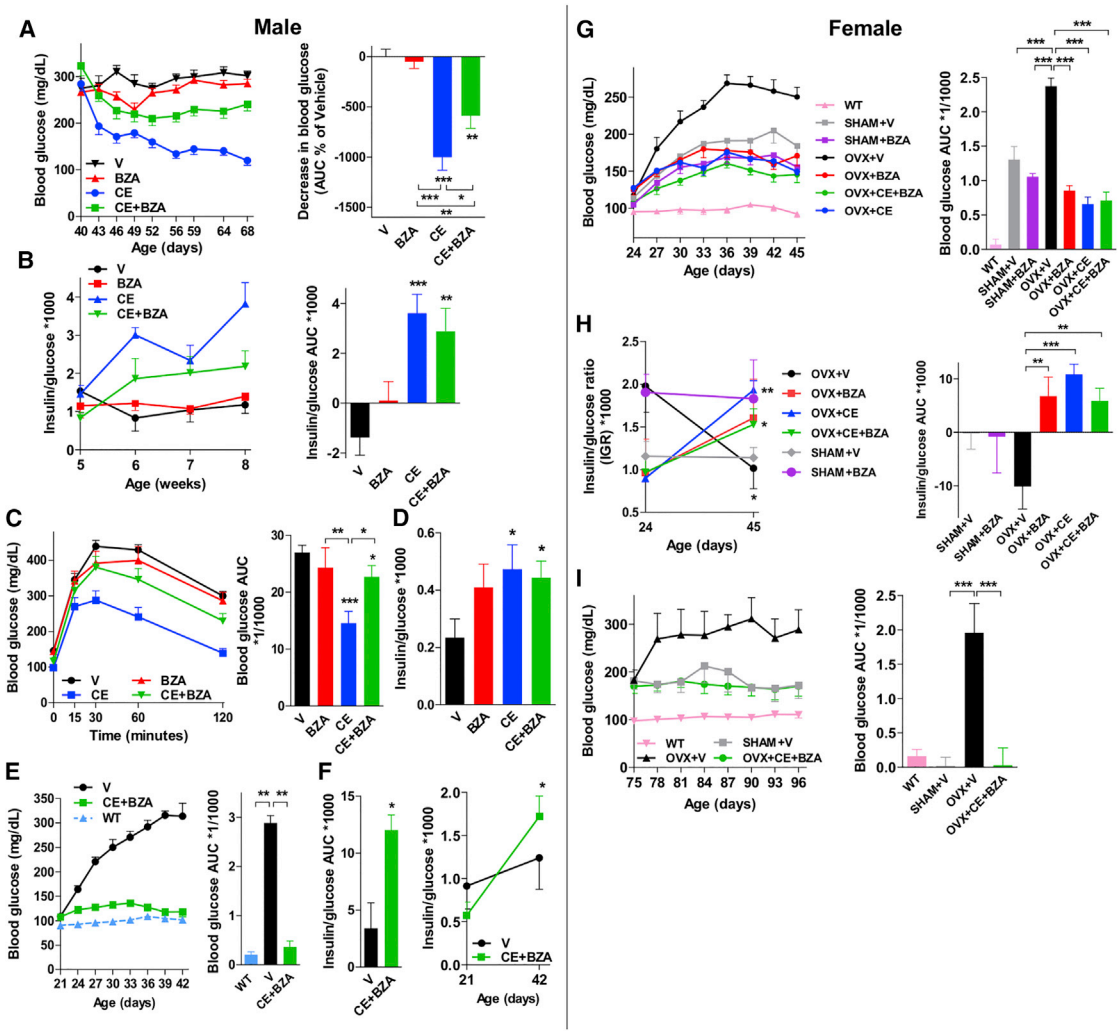

Figure 1. Effect of CE and BZA on Diabetes in Akita Mice

(A) Random-fed blood glucose (and corresponding AUC) in male Akita mice treated with vehicle, CE, BZA, or CE+BZA at the indicated age (n = 10–11 distinct animals/condition).

(B) Insulin/glucose ratio with corresponding AUC measured in mice from (A).

(C) IP-GTT with corresponding AUC in 8-week-old male Akita mice from (A).

(D) Insulin/glucose ratio at 30 min from the GTT in mice from (C).

(E) Random-fed blood glucose and corresponding AUC measured in young male WT and Akita mice treated with V or CE+BZA (n = 4–5 distinct animals/condition).

(F) Plasma insulin/blood glucose ratio in mice from (E).

(G) Random-fed blood glucose (and corresponding AUC) in OVX or sham-operated female Akita mice treated with compounds (n = 5–9 distinct animals/condition).

(H) Insulin/glucose ratio and corresponding AUC in mice from (G).

(I) Random-fed blood glucose and corresponding AUC in mature OVX or sham-operated female Akita mice treated with vehicle or CE/BZA (n = 4–5 distinct animals/condition).

Data are shown as mean ± SEM. *p < 0.05; **p < 0.01; and ***p < 0.001.

cultured male Ins2$^{+/Akita}$ insulinoma cells derived from male Akita β cells (Tsutsumi et al., 2004) and dispersed islet cells from female Akita mice. We exacerbated protein misfolding and ER stress pharmacologically *in vitro* using low-dose thapsigargin (Tg), an inhibitor of the sarco/endoplasmic reticulum Ca^{2+} ATPase (SERCA). Treatment with Tg decreases ER Ca^{2+}, inhibiting Ca^{2+}-dependent chaperone activity in the ER and promoting misfolded protein accumulation (Rogers et al., 1995). We quantified the expression of the proapoptotic component of the UPR, C/EBP homologous protein (CHOP) (Oyadomari and Mori, 2004). Exposure to Tg increased CHOP immunoreactivity and expression in male and in female Akita cells (Figures 3A–3C). Consistent with results obtained Akita mice, in Tg-exposed female Akita β cells, treatment with CE,

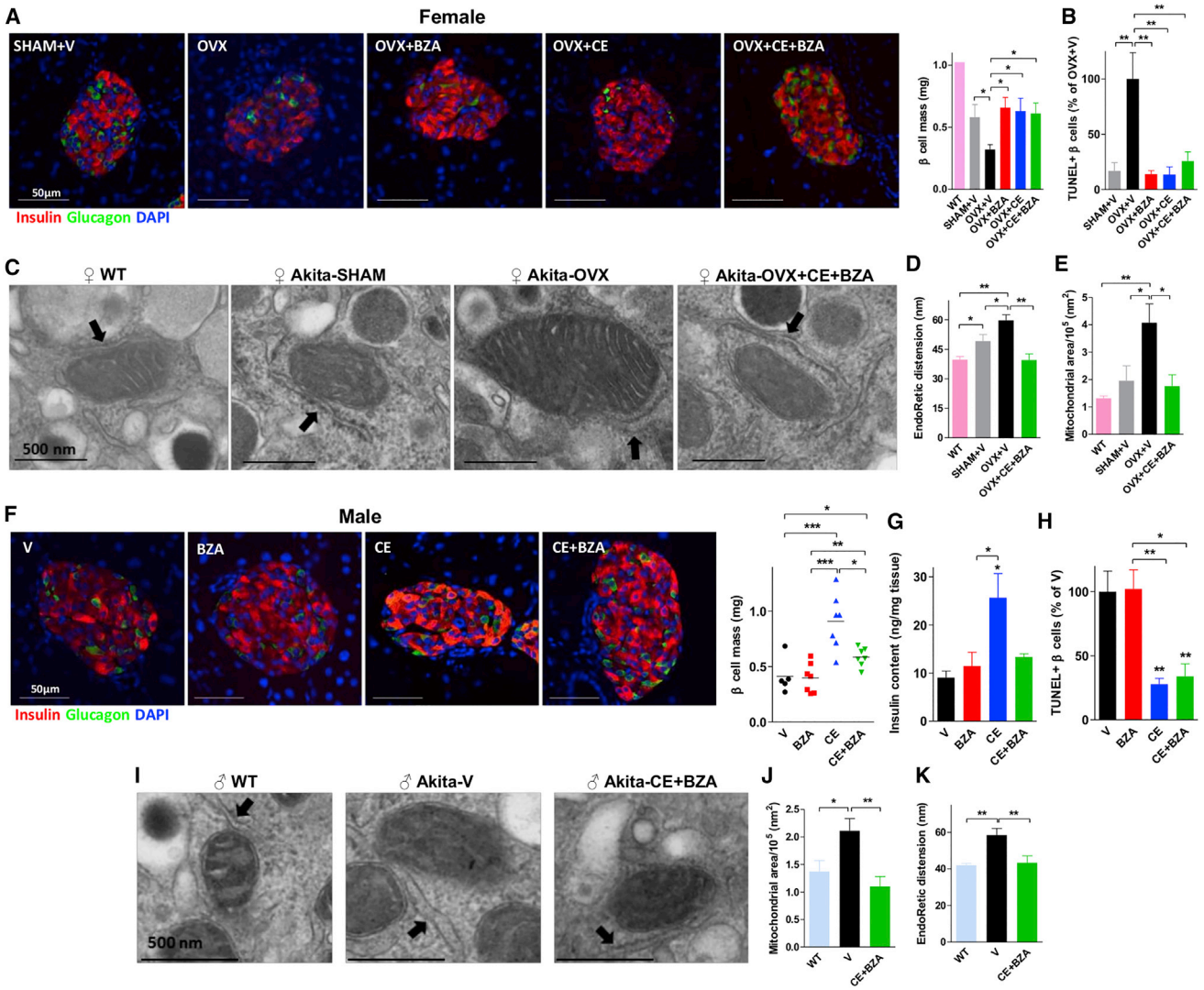

Figure 2. Effect of CE and BZA on β Cell Mass in Akita Mice

(A) Representative immunofluorescent (IF) staining of islets from OVX and sham-operated female Akita mice stained for insulin (red), glucagon (green), and nuclei (blue) and β cell mass quantification in mice from Figure 1G at 45 days.

(B) β cell apoptosis quantification by TUNEL staining in islet sections from (A) (n = 3 distinct animals/condition).

(C) Representative TEM images of mitochondria and ER from β cells of 3-week-old female WT and Akita mice treated with CE+BZA for 6 days.

(D and E) Quantification of the area of mitochondria (D) and dilation of ER (E) in mice from (C) (n = 4).

(F) Representative immunohistochemistry (IHC) staining of islets from male Akita mice stained for insulin (red), glucagon (green), and nuclei (blue) and β cell mass quantification in mice from Figure 1A at 68 days (n = 5–7 distinct animals/condition).

(G) Pancreatic insulin content in male Akita mice from (F) (n = 3–4).

(H) β cell apoptosis quantification in mice of (F) (n = 3–4).

(I) Representative TEM images of mitochondria and ER from β cells of 3-week-old male WT and Akita mice treated with vehicle or CE+BZA for 3 days.

(J and K) Quantification of the area of mitochondria (J) and ER dilation (K) in mice from (I) (n = 4 distinct animals/condition).

Data are shown as mean ± SEM. *p < 0.05; **p < 0.01; and ***p < 0.001.

BZA, and CE+BZA significantly decreased nuclear CHOP immunoreactivity (Figure 3A). In contrast, in Tg-exposed male Ins2$^{+/Akita}$ cells, CE and CE+BZA, but not BZA alone, decreased Tg-induced expression of CHOP (Figures 3B and 3C).

The UPR comprises three arms, mediated by three transmembrane ER proximal sensors of unfolded proteins, activating transcription factor 6 (ATF6), inositol-requiring transmembrane kinase/endonuclease 1α (IRE1α), and pancreatic ER kinase (PERK) (Figure 3D). We studied the effect of estrogens on each UPR arm in Tg-exposed Ins2$^{+/Akita}$ cells using the following UPR markers: immunoglobulin heavy chain-binding protein (BiP) for ATF6 activation, spliced X-box binding protein-1 (sXBP-1) mRNA for IRE1α activation, and activating

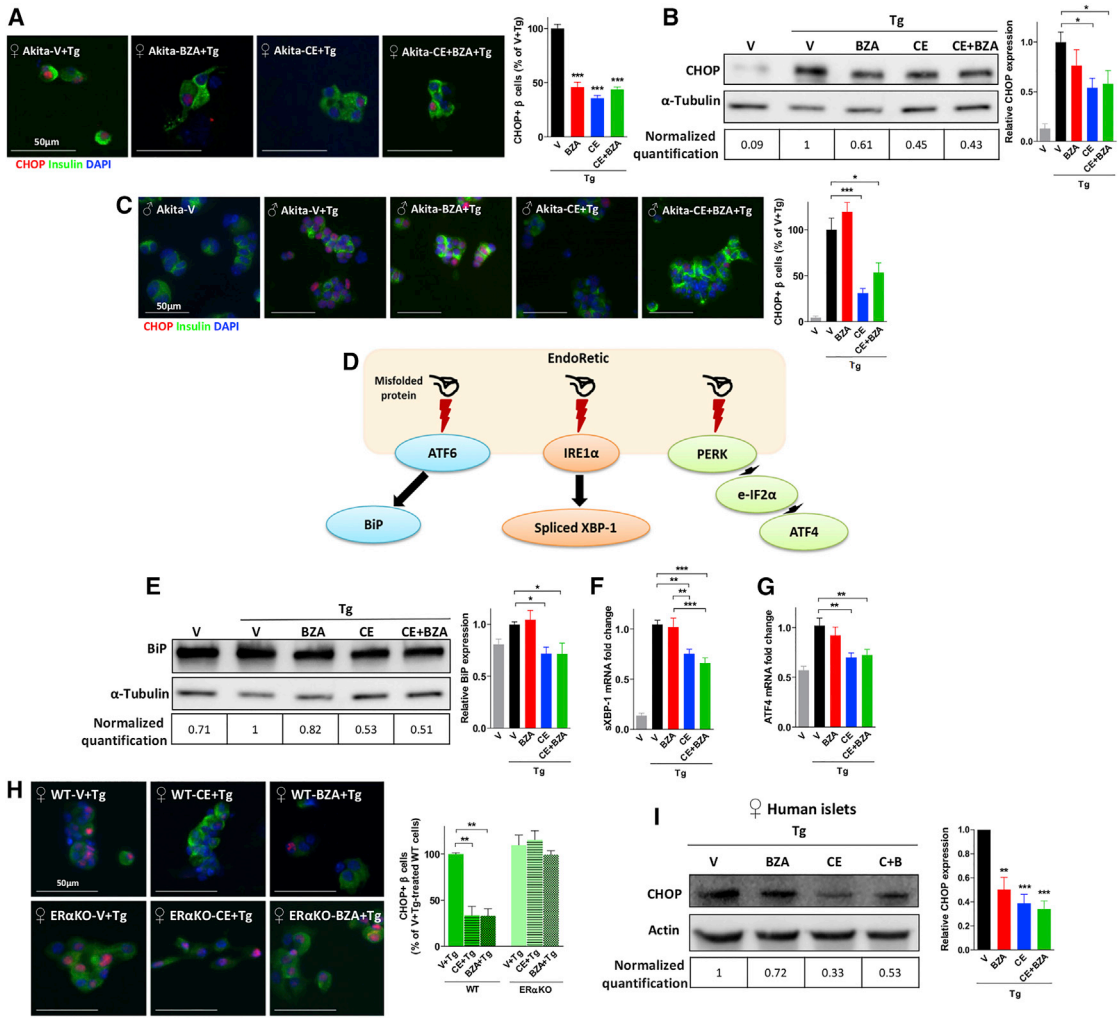

Figure 3. Effects of CE and BZA on ER Stress in Ins2$^{+/Akita}$ β Cells and Human Islets

(A) Dispersed islets from female Akita mice were treated with the indicated compounds for 24 hr, followed by exposure to Tg for 4 hr. Representative images of IF staining for CHOP (red), insulin (green), and nuclei (blue) and quantification of β cells with CHOP$^+$ nuclei relative to vehicle (n = 5 distinct experiments).

(B) Western blot of CHOP expression with quantification by densitometry in male Ins2$^{+/Akita}$ cells treated like in (a) (n = 6 distinct experiments).

(C) Male Ins2$^{+/Akita}$ β cells were treated like in (a). Representative images of IF staining for CHOP (red), insulin (green), and nuclei (blue) and quantification of β cells with CHOP$^+$ nuclei relative to vehicle (n = 6 distinct experiments).

(D) Schematic representation of three arms of the UPR.

(E) Male Ins2$^{+/Akita}$ cells were treated like in (A). Representative western blot for BiP and relative BiP protein expression levels quantified by densitometry (n = 4 experiments).

(F and G) qRT-PCR quantification of spliced XBP-1 mRNA (F) and ATF4 mRNA in male Ins2$^{+/Akita}$ cells (G) treated like in (A) (n = 8–9 distinct experiments).

(H) Dispersed islets from female WT and ERαKO mice were treated like in (A). Representative images of IF staining for CHOP (red), insulin (green), and nuclei (blue) and quantification of β cells with CHOP$^+$ nuclei relative to vehicle (n = 3 distinct experiments).

(I) Human islets from female donors were cultured like in (A). Representative western blot for CHOP protein expression levels and quantification (n = 3 distinct donors).

Data are shown as mean ± SEM. *p < 0.05; **p < 0.01; and ***p < 0.001.

transcription factor 4 (ATF4) mRNA and elf2α phosphorylation for PERK activation (Figure 3D). Treatment with CE or CE+BZA, but not BZA alone, decreased Tg-induced protein expression of BiP (Figure 3E), the mRNA expression of sXBP-1 (Figure 3F) and ATF4 (Figure 3G). CE also decreased Tg-induced phosphorylation of elf2α (Figure S3A). Together, these results confirm results obtained with CHOP that CE help resolve UPR in these cells.

CE and BZA Protect Female Akita β Cells against ER Stress via ERα

Three estrogen receptors are expressed in β cells: ERα, ERβ, and the G-protein-coupled estrogen receptor (GPER). To determine which receptor(s) is (are) involved in the protective role of CE and BZA against ER stress in female mice, we studied dispersed islets of female ERα knockout (ERαKO), ERβ knockout (ERβKO). and GPER knockout (GPERKO) mice and their corresponding

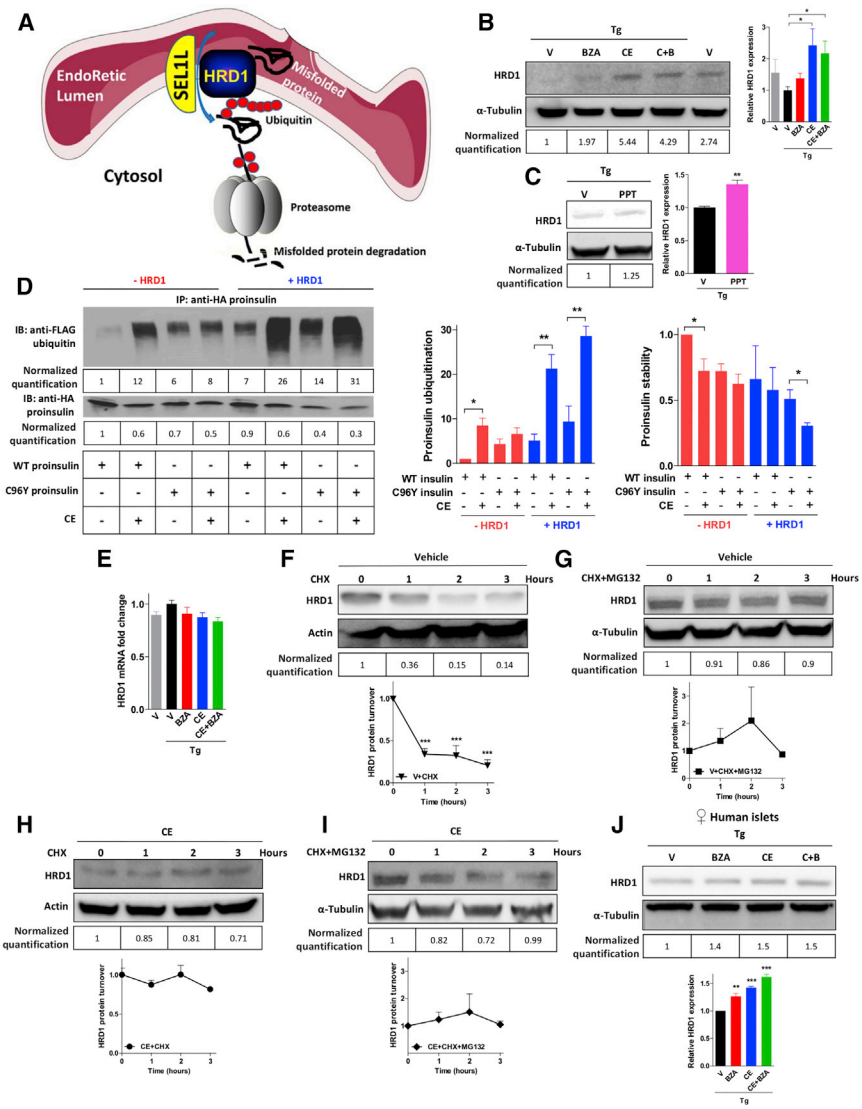

Figure 4. CE-ERα Promotes Misfolded Proinsulin Degradation via HRD1-ERAD Stabilization

(A) Diagram of misfolded protein degradation via ERAD including misfolded protein retrotranslocation to the cytosol via E3 ubiquitin ligase HRD1 and its scaffold adaptor SEL1L followed by HRD1-mediated ubiquitination and proteasomal degradation.

(B and C) Male Ins2$^{+/Akita}$ cells were treated with CE and BZA (B) or PPT (C) for 24 hr, followed by exposure to Tg for 4 hr. Representative image of western blot for HRD1 expression and quantification (n = 4–7 distinct experiments/condition).

(D) COS-7 cells were transfected with HA-WT proinsulin or HA-C96Y proinsulin along with ERα and FLAG-ubiquitin in the absence or presence of HRD-1. Cells were treated with CE for 24 hr, followed by exposure to Tg for 4 hr. Co-immunoprecipitations were carried out using anti-HA antibody followed by western blotting using anti-FLAG or anti-HA antibodies (left). Quantification of relative proinsulin ubiquitination (middle) and proinsulin stability (right) (n = 3 distinct experiments/condition).

(E) Male Ins2$^{+/Akita}$ cells were treated like in (B), followed by qRT-PCR quantification of HRD1 mRNA (n = 8 experiments).

(F–I) Male Ins2$^{+/Akita}$ cells were treated with cycloheximide (CHX) plus Tg and either vehicle (F and G) or CE (H and I) in the presence (G and I) or in the absence (F and H) of MG132 for the indicated time course. Western blots for HRD1 were performed on cell lysates. Relative HRD1 protein levels were determined by densitometry and were normalized to that obtained at time 0 (n = 4–6 distinct experiments/condition).

(J) Islets from female human donors were treated like in (B). Representative image of western blot for HRD1 expression and bar graph of quantification (n = 3).

Data are shown as mean ± SEM. *p < 0.05; **p < 0.01; and ***p < 0.001.

WT littermates. The protective effect of CE and BZA against Tg-induced CHOP nuclear expression in WT β cells was abolished in ERαKO β cells (Figure 3H), but not in ERβKO and GPERKO β cells (Figures S3B and S3C), indicating that ERα was indispensable for CE and BZA prevention of ER stress in female β cells. Importantly, CE, BZA, and CE+BZA also suppressed Tg-induction of CHOP expression in cultured islets obtained from adult human female organ donors (Figure 3I).

CE Activation of ERα Promotes Misfolded Proinsulin Degradation by Stabilizing the ER-Associated Protein Degradation System

We reasoned that if activation of ERα protects β cells from ER stress in the presence of mutant Akita proinsulin, it may promote misfolded proinsulin degradation. The ER-associated protein degradation (ERAD) pathway plays a critical role in cellular proteostasis by removing unfolded proteins via retrograde transport from the ER back to the cytosol, where these unfolded proteins are degraded by the ubiquitin-proteasome system (Qi et al., 2017; Smith et al., 2011). The major instrument of the ERAD in mammals is the hydroxymethylglutaryl reductase degradation protein 1 (HRD1), an E3 ubiquitin ligase located in the ER membrane (Figure 4A) (Kaneko et al., 2010; Qi et al., 2017; Smith et al., 2011). We used male Ins2$^{+/Akita}$ cells to study the effect of CE on ERAD, as the absence of an equivalent cell line in females precludes detailed molecular studies of the mechanisms. In Ins2$^{+/Akita}$ cells exposed to Tg, treatment with CE and CE+BZA, but not BZA alone, increased HRD1 protein expression, and this was reproduced by the selective ERα agonist PPT (Figures 4B and 4C), suggesting that HRD1 is the effector activated by CE-ERα to promote the ubiquitination of misfolded insulin. HRD1 can promote the ubiquitination of misfolded Akita C^{96}Y proinsulin in COS-7 cells (Allen et al., 2004). To ascertain whether HRD1 is instrumental in CE's ability to promote the ubiquitination

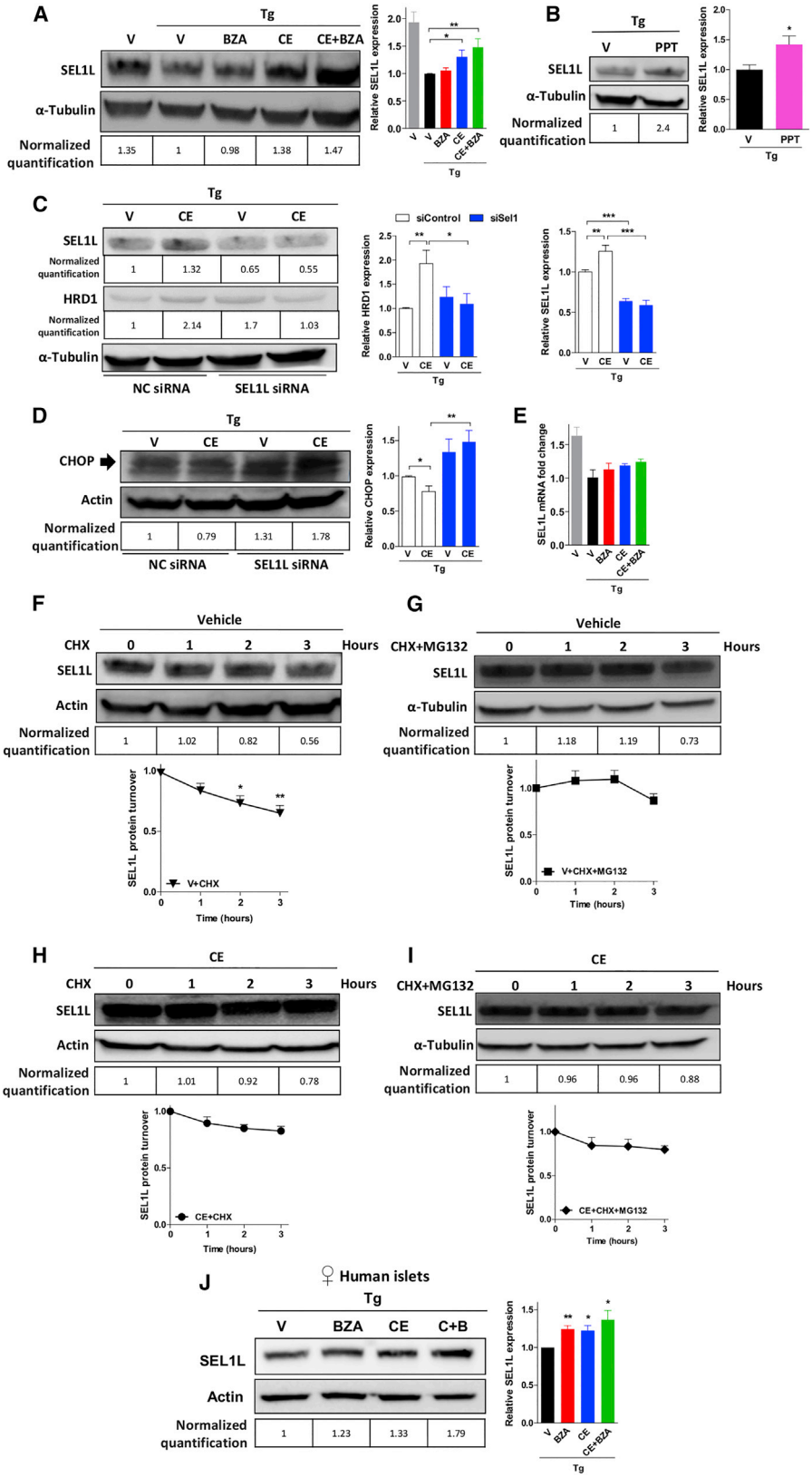

(legend on next page)

and degradation of $C^{96}Y$ proinsulin, we co-transfected COS-7 cells with ERα, HRD1, and ubiquitin and either WT or $C^{96}Y$ proinsulin. In this cellular system, in the absence of HRD1 there were slightly higher levels of ubiquitin modification of WT compared to $C^{96}Y$ proinsulin (Figure 4D), and CE promoted a modest reduction in WT proinsulin levels (Figure 4D). Most importantly, in the presence of HRD1, CE increased ubiquitin modification of WT and $C^{96}Y$-proinsulin with a relatively larger increase in HRD1-mediated ubiquitin modification of $C^{96}Y$-proinsulin (Figure 4D). As a result, in the presence of HRD1, CE increased $C^{96}Y$-proinsulin destabilization without affecting WT proinsulin stability (Figures 4D and S4). Thus, in the presence of HRD1, CE preferentially promote the degradation of misfolded C96Y-proinsulin.

Interestingly, in $Ins2^{+/Akita}$ cells exposed to ER stress, CE increased HRD1 protein without increasing HRD1 mRNA levels (cf. Figures 4B–4E), suggesting that CE promote HRD1 protein stabilization via post-translational mechanisms. To determine to what extent CE treatment stabilizes HRD1 protein, we studied HRD1 protein turnover in the presence of the protein synthesis inhibitor cycloheximide (CHX) to block *de novo* protein synthesis. In the absence of CE, HRD1 was rapidly degraded (Figure 4F), and this was blocked by the proteasome inhibitor MG132, demonstrating that HRD1 turnover is dependent on proteasomal degradation (Figure 4G). However, CE treatment stabilized HRD1 protein expression (Figure 4H), and this was unaltered by proteasome inhibition (Figure 4I), demonstrating that CE prevent HRD1 proteasomal degradation. Notably, treatment with CE, BZA, and the combination CE+BZA also stabilized HRD1 protein expression in Tg-exposed cultured islets obtained from human female donors (Figure 4J).

The suppressor/enhancer of Lin-12-like (SEL1L) is a membrane adaptor protein that acts as a scaffold for HRD1 (Figure 4A) (Iida et al., 2011). Acute conditional SEL1L knockdown in mice results in a rapid degradation of HRD1 protein in the pancreas, demonstrating that SEL1L promotes HRD1 protein stability *in vivo*. We tested the possibility that activation of ERα stabilizes HRD1 via increasing SEL1L. In $Ins2^{+/Akita}$ cells exposed to Tg, treatment with CE and the ERα agonist PPT (but not BZA alone) increased SEL1L protein compared to vehicle treatment (Figures 5A and 5B). We wondered whether SEL1L is instrumental in the effect of CE-ERα to protect β cells via stabilization of HRD1 following SEL1L small interfering RNA (siRNA) knockdown in $Ins2^{+/Akita}$ cells. Following a 50% knockdown of SEL1L protein, the ability of CE to stabilize HRD1 protein expression was abolished (Figure 5C), and, as a result, the ability of CE to suppress CHOP protein expression was blocked (Figure 5D), together demonstrating that SEL1L is instrumental in the ability of CE to stabilize HRD1 protein and mitigate ER stress. Like in the case of HRD1, CE increased SEL1L protein in $Ins2^{+/Akita}$ cells exposed to Tg without increasing SEL1L mRNA levels (Figure 5E), suggesting that CE also promote the stabilization of SEL1L protein. We assessed SEL1L protein turnover like in the case of HRD1. In the absence of CE, SEL1L was progressively degraded (Figure 5F) by proteasomal degradation (Figure 5G). However, CE prevented SEL1L proteasomal degradation (Figures 5H and 5I). Importantly, treatment with CE, BZA, and the combination CE+BZA also stabilized SEL1L protein in Tg-exposed cultured islets obtained from human female donors (Figure 5J). Of note, Tg decreases SEL1L mRNA and protein, suggesting that ER stress itself alters SEL1L expression (Figures 5A and 5E).

Membrane and Nuclear ERα Stabilize the ERAD by Inhibiting the Ubiquitin-Conjugating Enzyme UBC6e

The E2 ubiquitin-conjugating enzyme UBC6e (*Ube2j1* gene) is the only UBC to localize to the ER and to physically interact via its transmembrane domain with SEL1L (Burr et al., 2011; Hagiwara et al., 2016). In fact, UBC6e is considered an ERAD degrader, and UBC6e KO mouse embryo fibroblasts exhibit increased expression of SEL1L (Hagiwara et al., 2016) (like CE-treated cells). Therefore, we investigated the possibility that UBC6e is ERα's primary target in the stabilization of the SEL1L-HRD1 ERAD complex. In $Ins2^{+/Akita}$ cells exposed to Tg, treatment with CE and the ERα agonist PPT suppressed UBC6e mRNA suggesting that CE activation of ERα suppresses UBC6e gene transcription (Figure 6A). Further, consistent with previous data described above, BZA suppressed UBC6e mRNA in female WT mouse islets, but had no effect in age-matched male islets (Figure 6B). Note that Tg increased UBC6e mRNA, suggesting that ER stress itself increases UBC6e gene expression (Figure 6B). Importantly, the ability of CE, BZA, and the combination CE+BZA to decrease UBC6e protein expression was translated to Tg-exposed cultured islets obtained from adult human female donors (Figure 6C). To confirm that downregulation of UBC6e was instrumental in the ability of CE-ERα to stabilize ERAD proteins and protect β cells from chronic ER stress, we overexpressed UBC6e in $Ins2^{+/Akita}$ cells. Following a 2-fold increase in UBC6e protein expression (which was unresponsive to suppression by CE), the basal expression of HRD1 and SEL1L proteins was decreased and the ability of

Figure 5. CE-ERα Prevents HRD1 Degradation and ER Stress via SEL1L Stabilization

(A and B) Male $Ins2^{+/Akita}$ cells were treated with CE and BZA (A) or PPT (B) for 24 hr, followed by exposure to Tg for 4 hr. Representative image of western blot for SEL1L expression and bar graph of quantification (n = 4–8 distinct experiments/condition).

(C and D) Male $Ins2^{+/Akita}$ cells were transfected with mouse SEL1L-specific siRNA or with a control siRNA and were treated like in (A). Protein expression for SEL1L, HRD1 (C), and CHOP (D) were analyzed by western blotting and quantification (n = 4–6 experiments).

(E) Male $Ins2^{+/Akita}$ cells were treated like in (A) and qRT-PCR quantification of relative SEL1L mRNA was performed and represented as expression relative to vehicle+Tg. n = 8–9 distinct experiments/condition.

(F–I) Male $Ins2^{+/Akita}$ cells were treated with cycloheximide (CHX) plus Tg and vehicle (F and G) or CE (H and I) in the presence (G and I) or absence (F and H) of MG132 for the indicated time course. SEL1L protein was quantified by western blot and relative SEL1L protein levels were determined by densitometry and normalized to that obtained at time 0 (n = 4–6 distinct experiments/condition).

(J) Islets from female human donors were treated like in (A). Representative image of western blot for SEL1L protein expression and bar graph of quantification (n = 3 experiments).

Data are shown as mean ± SEM. *p < 0.05, **p < 0.01, ***p < 0.001.

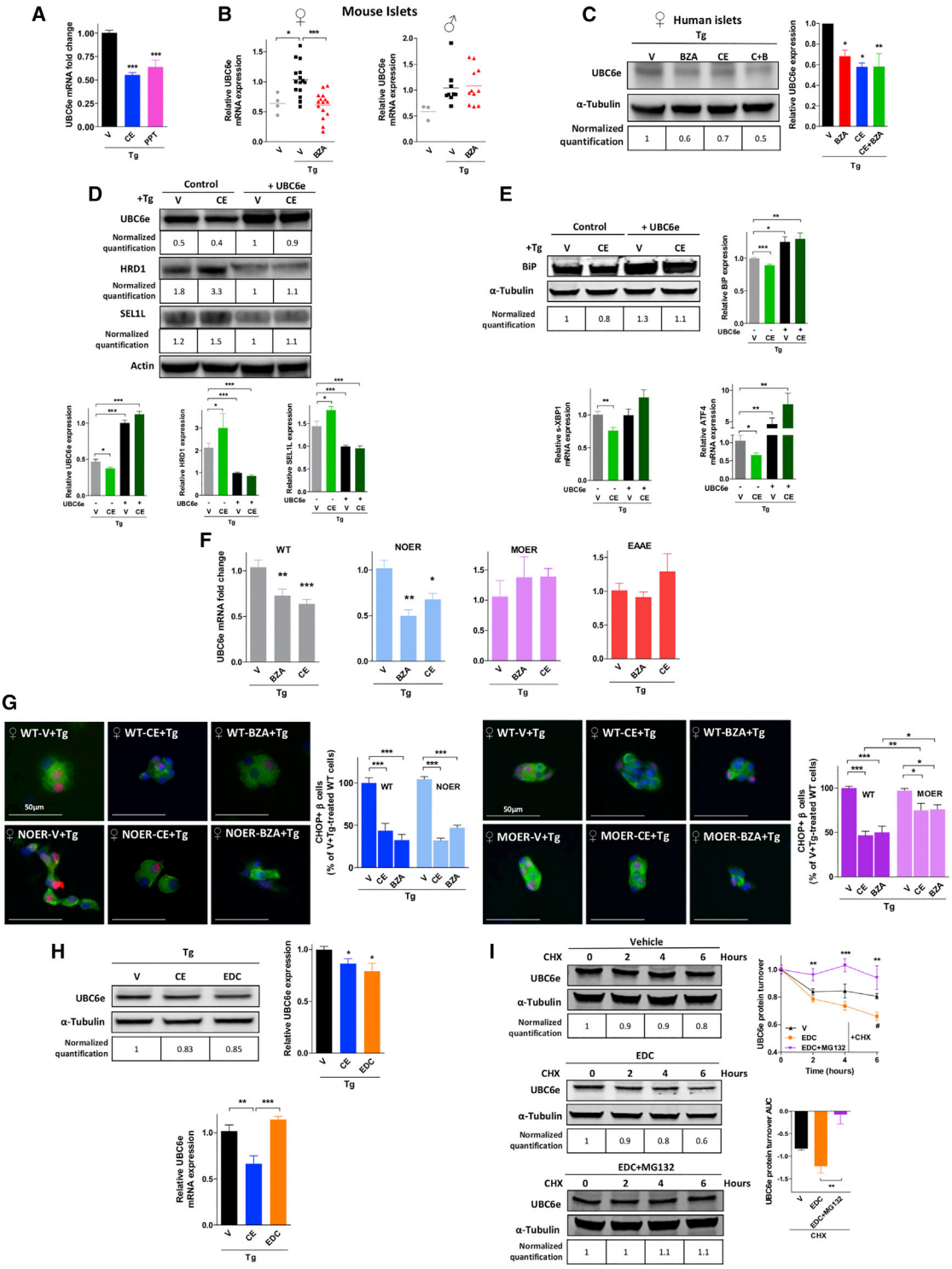

Figure 6. CE-ERα Stabilizes ERAD in β Cells by Inhibiting UBC6e

(A) Male Ins2$^{+/Akita}$ cells were treated with the indicated compounds for 24 hr followed by exposure to Tg for 4 hr. qRT-PCR quantification of relative UBC6e mRNA levels is shown (n = 8 experiments/condition).

(B) Female and male WT mouse islets were treated with BZA for 24 hr followed by exposure to Tg for 4 hr, and UBC6e mRNA level were quantified by qRT-PCR (n = 9–15 distinct experiments/condition).

(C) Islets from female human donors were treated like in (A). Western blot for UBC6e protein expression and bar graph of quantification (n = 3 experiments).

(legend continued on next page)

CE to stabilize HRD1 and SEL1L was abolished (Figure 6D), demonstrating that UBC6e is a critical target of ERα to stabilize the ERAD complex. Further, following UBC6e overexpression, the basal expression of UPR sensors was increased, and the ability of CE to suppress the expression of BiP protein, s-XBP-1 and ATF4 mRNAs was abolished (Figure 6E), confirming that UBC6e is instrumental in the ability of CE to resolve the activation of the three arms of the UPR. We next investigated the mechanism by which CE-ERα suppresses UBC6e. Pools of nuclear or membrane ERα can mediate estrogens' actions in β cells (Tiano and Mauvais-Jarvis, 2012). To assess the contribution of nuclear ERα, we used a knockin mouse with mutant ERα that precludes ERα palmitoylation and membrane localization. In this "nuclear only ERα" (NOER) mouse, ERα is exclusively nuclear, and membrane/extranuclear actions of ERα are abolished (Pedram et al., 2014, 2015). In contrast, we also used an ERα-deficient mouse re-expressing ERα selectively at the plasma membrane, the membrane-only estrogen receptor-α (MOER) mouse (Pedram et al., 2009). In islet cells from female WT and NOER mice exposed to Tg, treatment with CE or BZA decreased UBC6e mRNA (Figure 6F) and accordingly CE and BZA completely suppressed CHOP nuclear expression (Figure 6G). However, the effect of CE or BZA to suppress UBC6e mRNA expression and CHOP nuclear expression was, respectively, abolished and reduced in MOER cells (Figures 6F and 6G). Thus, CE and BZA suppress UBC6e gene expression in β cells and protect against ER stress mainly through nuclear ERα signaling (and partially via membrane ERα signaling). Next, we sought to determine to what extent nuclear ERα requires ERα binding an estrogen-response element (ERE) on the promoter of the UBC6e gene (*Ube2j1*). We used the ERα DNA-binding domain mutant mouse (ERα-EAAE), which does not support E_2-mediated transcription and lacks the ability to bind perfect consensus EREs, 1-nt variant EREs, and a small subset of 2-nt variant EREs (Hewitt et al., 2014). In islet cells from female EAAE mice exposed to Tg, treatment with CE or BZA failed to suppress UBC6e mRNA expression compared to WT islets, demonstrating that ERα suppresses *Ube2j1* via a nuclear receptor functional enhancer (NRFE) ERE (Figure 6F) (Coons et al., 2017). Next, we looked at locations of EREs on the chromosome that contains the *Ube2j1* gene in the mouse and human genome. No NRFE ERE is present in the promoter of *Ube2j1* in either the mouse or human genome (Figure S5). The closest perfect ERE is located ~400 kb upstream to the transcription start site (TSS) of *Ube2j1* in the mouse genome and ~500 kb in the human genome. The closest 1-nt variant EREs are located 12 and 88 kb upstream of the TSS of *Ube2j1* (Figure S5), respectively. Thus, CE suppress UBC6e via ERα acting on a NRFE ERE, likely in a distant enhancer, but not on the *Ube2j1* promoter.

That CE and BZA each failed to suppress UBC6e mRNA but partially suppressed CHOP activation in female MOER β cells (cf. Figures 6F and 6G) suggested that membrane ERα may also help resolve ER stress independently from suppressing *Ube2j1* transcription. To address this issue, we used an estrogen dendrimer conjugate (EDC) that remains outside the nucleus and is the gold standard for studying extra-nuclear ERα actions (Chambliss et al., 2010; Harrington et al., 2006). In $Ins2^{+/Akita}$ cells, EDC, like CE, suppressed UBC6e protein expression (Figure 6H). However, unlike CE, EDC failed to suppress UBC6e mRNA (Figure 6H), suggesting that ERα extranuclear actions promote UBC6e protein degradation. To address this issue, we studied UBC6e protein turnover. Compared to vehicle, EDC treatment destabilized UBC6e protein (Figure 6I), and this was abolished by proteasome inhibition (Figure 6I). Together, this demonstrates that EDC activation of extranuclear ERα promotes UBC6e proteasomal degradation.

BZA Antagonizes ERα Action on EREs in Male β Cells

BZA suppresses β cell apoptosis and protects functional β cell mass, thus preventing the onset of diabetes in OVX female Akita mice (Figures 1 and 2). However, BZA does not provide β cell protection in adult male Akita mice and even reverses the effect of CE (Figures 1 and 2). Further, BZA suppresses ER stress via ERα in cultured female Akita β cells, but not in male Akita β cells (Figure 3). Therefore, unlike CE and E2, which are pure ERα agonists in β cells from both sexes, BZA is an ERα agonist selectively in female β cells. In male $Ins2^{+/Akita}$ cells, CE's agonist action on ERα decreases the activation of the UPR markers BiP, ATF4, and sXBP-1 and as a result suppresses CHOP expression (Figure 3). In addition, CE suppress UBC6e mRNA and protein expression and therefore stabilizes HRD1 and SEL1L from proteasomal degradation (Figures 4, 5, and 6). In contrast, in male $Ins2^{+/Akita}$ cells, BZA does not suppress UPR pathways (Figure 3), does not decrease UBC6e expression (Figure 6B) and does not stabilize SEL1L-HRD1 ERAD proteins (Figures 4, 5, and 6), suggesting that BZA is an ERα antagonist in male β cells.

We first explored the possibility that BZA could be a selective estrogen receptor degrader (SERD) in male β cells. The ERα is a short lived protein whose stability is influenced by the nature of

(D) Male $Ins2^{+/Akita}$ cells were transfected with mouse UBC6e or control expression plasmids and treated like in (A). Western blot for UBC6e, SEL1L, and HRD1 protein expression (upper panel) and bar graph of quantification (lower panel) are shown (n = 4–10 distinct experiments/condition).
(E) Male $Ins2^{+/Akita}$ cells were transfected with mouse UBC6e or control plasmids and treated like in (A). Western blot for BiP protein (upper panel) and bar graph of qRT-PCR quantification of spliced-XBP1 and ATF4 mRNAs (lower panel) (n = 6 distinct experiments/condition).
(F) Cultured islets from female WT, NOER, MOER, and EAAE mice were treated like in (A), followed by qRT-PCR quantification of relative UBC6e mRNA levels (n = 6 distinct experiments/condition).
(G) Dispersed islets from female WT, MOER, and NOER mice were treated like in (A). Images of IF staining for CHOP, insulin, and nuclei and quantification of β cells with $CHOP^+$ nuclei relative to vehicle (n = 4–6 experiments).
(H) Male $Ins2^{+/Akita}$ cells were treated with the indicated compounds for 24 hr, followed by exposure to Tg for 4 hr. Protein expression (upper panel) and mRNA level (lower panel) of UBC6e (n = 6–10 distinct experiments/condition).
(I) Male $Ins2^{+/Akita}$ cells were treated with CHX plus Tg and either vehicle or EDC in the presence or in the absence of MG132 for the indicated time course. UBC6e protein was measured by western blot and relative UBC6e protein levels were determined by densitometry and were normalized to that obtained at time 0 (n = 3–6 experiments).

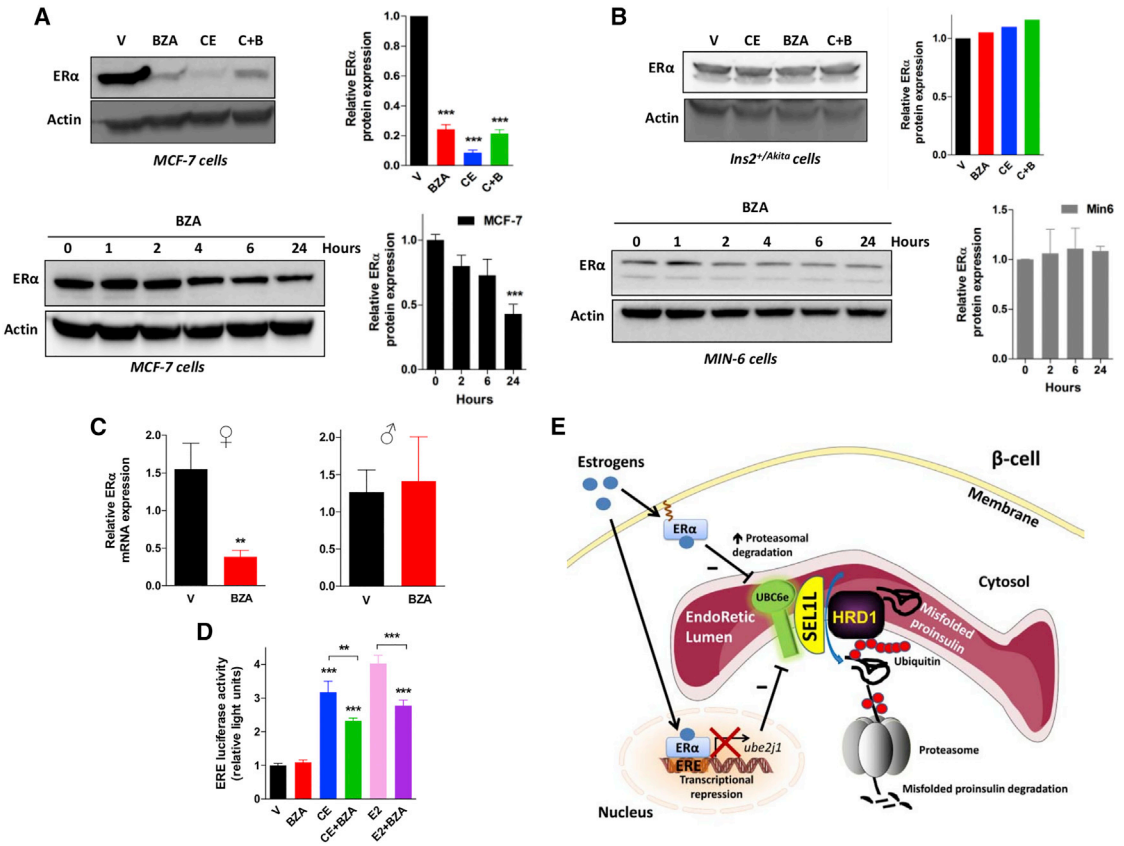

Figure 7. BZA Antagonizes ERα Actions in Male β Cells

(A) MCF-7 cells were treated with vehicle, CE (10^{-7} M), BZA (10^{-6} M), or CE+BZA for 24 hr (upper panel). MCF-7 cells were treated with BZA (10^{-6} M) for the indicated time points during 24 hr (lower panel). Cell lysates were subjected to western blot using anti-mouse ERα antibody. Quantification by densitometry is shown in adjacent bar graph (n = 4).

(B) Ins2$^{+/Akita}$ cells (upper panel) were treated with vehicle, CE (10^{-7} M), BZA (10^{-6} M), or CE+BZA for 24 hr (upper panel). MIN6 cells (lower panel) were treated with BZA (10^{-6} M) for the indicated time points during 24 hr (n = 4). Cell lysates were treated like in (A).

(C) Female and male WT mouse cultured islets were treated with BZA for 24 hr like in (A), and the ERα mRNA levels were quantified by qRT-PCR in the indicated groups (n = 9–12 distinct experiments/condition).

(D) MIN6 cells were transfected with ERE-Luc plasmid, followed by treatment with the indicated compounds and quantification of luciferase activity (n = 4–10 experiments distinct experiments/condition). Data are shown as mean ± SEM. *p < 0.05; **p < 0.01; and ***p < 0.001.

(E) Proposed mechanism for ERα activation of ERAD in β cells. Estrogens activation of nuclear ERα promote transcriptional repression of the UBC6e gene via an ERE, whereas estrogens activation of membrane ERα promote the proteasomal degradation of UBC6e protein. The resultant decrease in UBC6e protein expression and activity stabilizes SEL1L, which, in turn, stabilizes HRD1 and promotes the proteasomal degradation of misfolded insulin. This results in increased HRD1-mediated ubiquitination and proteasomal degradation of misfolded proinsulin.

the bound ligand (Wijayaratne and McDonnell, 2001). The half-life of ERα in both breast and uterine tissues in the absence of ligand is 5 hr. However, upon binding E_2 or the pure ER antagonist fulvestrant, the half-life of mouse ERα decreases to 2 and 0.5 hr, respectively (Dauvois et al., 1992). SERDs are drugs that bind to and induce a conformational change in ERα that targets it for proteasomal degradation in breast tissue. BZA is a pure ERα antagonist in breast but is also a SERD, because BZA degrades ERα in breast cells, thus eliminating its target (Wardell et al., 2013). To determine whether BZA is a SERD in male β cells, we studied ERα protein turnover in male Ins2$^{+/Akita}$ cells (Wijayaratne and McDonnell, 2001). As previously described, BZA promoted ERα protein degradation in MCF-7 cells producing less than 50% protein expression within 24 hr (Figure 7A) (Wardell et al., 2013; Wijayaratne and McDonnell, 2001). In contrast, after 24-hr exposure, BZA did not alter ERα turnover and did not change ERα protein expression in Ins2$^{+/Akita}$ and MIN6 cells (Figure 7B).

Having established that BZA is not a SERD in male β cells, we sought to determine to what extent it is an ERα antagonist. Agonist-activated ERα downregulates the expression of its own gene (*Esr1*), via an ERE on the *Esr1* promoter (Tiano et al., 2015). Accordingly, BZA suppressed ERα mRNA in female WT mouse islets (Figure 7C). In contrast, BZA showed no effect on ERα mRNA in age-matched male islets (Figure 7C). Consistent with these results, in male Ins2$^{+/Akita}$ cells transfected with an ERE reporter construct, E_2 and CE activated ERE signaling (Figure 7D), but BZA had no effect on ERE activation. Further, and

consistent with BZA antagonizing ERα actions on EREs, BZA reversed CE and E_2 activation of the ERE (Figure 7D).

DISCUSSION

CE treatment mitigates ER stress in cultured Akita β cells and in male and female islets from Akita mice, thereby preventing β cell apoptosis, maintaining insulin secretion and delaying diabetes onset. CE prevention of β cell failure in Akita mice could be partially mediated via non-islet cells effects easing the metabolic stress on β cells. However, extensive evidence demonstrates that estrogens protect β cell survival and function *in vivo* in rodents and cultured human islets via direct effect on ERα in β cells (Kilic et al., 2014; Le May et al., 2006; Liu et al., 2009, 2013; Tiano et al., 2011; Tiano and Mauvais-Jarvis, 2012; Wong et al., 2010). Therefore, it is likely that in the Akita model of pure insulin deficiency, CE prevent diabetes via a direct β cell effect preventing ER stress. In fact, in Akita cells CE decrease nuclear expression of CHOP and suppresses the activation of UPR sensors ATF6, IRE1α, and PERK (assessed by their proximal markers BiP, sXBP-1, and ATF4, respectively), demonstrating that CE relieve the ER from the chronic stress of protein misfolding. Two mechanisms can minimize ER stress: a pre-emptive upregulation of the UPR to restore proteostasis or the suppression of the stress itself via either activation of chaperones or enhancement of the ERAD, decreasing misfolded protein accumulation. We find that CE stabilize the ERAD that promotes the proteasomal degradation of misfolded proteins. The importance of the ERAD in cellular health cannot be understated, since multiple human diseases are linked to ERAD failure (Qi et al., 2017). In Akita cells, the ERAD participates in the turnover of mutant $C^{96}Y$ proinsulin in the ER, but is not sufficiently activated to prevent apoptosis (He et al., 2015). We show that CE promote ERAD activation by stabilizing its main effector, the E3 ubiquitin ligase HRD1, which accelerates the ubiquitination and proteasomal degradation of misfolded $C^{96}Y$ proinsulin. Using a cellular system validated to compare mutant and WT proinsulin ubiquitination and degradation in the presence of HRD1 (Allen et al., 2004), we confirm that CE increase HRD1-mediated ubiquitination of $C^{96}Y$ proinsulin, which is associated with a selective $C^{96}Y$ proinsulin destabilization. Thus, in the presence of HRD1, CE promote the preferential degradation of misfolded C96Y over WT proinsulin, potentially decreasing the dominant-negative effect of C96Y proinsulin that prevents WT proinsulin from exiting the ER, and being secreted as insulin (Haataja et al., 2016). We show that CE treatment prevents SEL1L protein degradation, and this is critical to stabilize HRD1 protein. Indeed, when SEL1L protein expression is knocked down by 50% in Akita cells, CE fail to stabilize HRD1 protein and fails to prevent ER stress.

CE stabilizes the ERAD and mitigates ER stress in β cells via its main receptor ERα. In the absence of ERα, CE fail to suppress pharmacologically induced ER stress in cultured female islets. ERAD degraders prevent ERAD-mediated premature degradation of functional proteins that have not yet attained their folded conformation, and therefore HRD1 and SEL1L are short-lived proteins (Noack et al., 2014). CE activation of ERα stabilizes SEL1L and HRD1 proteins in Akita cells by preventing their proteasomal degradation by the ERAD degrader and ubiquitin-conjugating enzyme UBC6e. UBC6e is the only UBC to localize to the ER, and one of its main targets is SEL1L (Hagiwara et al., 2016). We show that CE activation of ERα in the nucleus of β cells promotes the transcriptional repression of the UBC6e gene via an ERE, and this is associated with decreased CHOP nuclear expression. However, CE acting on membrane pools of ERα also accelerates the proteasomal degradation of UBC6e protein. Therefore, in the absence of ERα activation (OVX Akita females), UBC6e protein expression is increased and stabilized in Akita β cells, which promotes SEL1L-HRD1 proteasomal degradation, allowing misfolded proinsulin accumulation. In the presence of estrogens, the activation of nuclear ERα suppresses the production of new UBC6e mRNA and protein, while the activation of membrane ERα promotes the degradation of existing UBC6e protein. Together these effects decrease UBC6e protein expression and activity, stabilizing the ERAD and restoring β cell proteostasis.

UBC6e inhibition is central to the effects of CE, as overexpression of UBC6e in Akita cells by only 2-fold (which prevents CE suppression of UBC6e) blocks the ability of CE to stabilize HRD1 and SEL1L, and to suppress the activation of the UPR. Importantly, in cultured islets from human female donors exposed to pharmacologically induced protein misfolding, treatment with CE, BZA, and the combination CE+BZA also suppresses UBC6e protein expression, stabilizes SEL1L-HRD1 proteins, and reduces CHOP protein, demonstrating the translational potential of this finding to protect β cells in women. We propose that the mechanism of estrogens' protection of β cell survival against gluco-lipotoxicity, proinflammatory cytokines, and oxidative stress (all conditions promoting ER stress) is a promotion of ERAD-mediated misfolded proinsulin degradation and promotion of β cell proteostasis via suppression of UBC6e (Figure 7E).

Another important finding is that bazedoxifene, a SERM that exhibits ERα antagonist activity in breast and uterus and is used in combination with CE during menopausal therapy, is an ERα agonist in female β cells. In contrast, bazedoxifene is an ERα antagonist on EREs in male β cells. In OVX female Akita mice, bazedoxifene decreases β cell apoptosis thus preventing the onset of diabetes. Further, bazedoxifene suppresses ER stress in cultured female Akita β cells. The combination of CE with bazedoxifene has similar protective activity in female cultured β cells and *in vivo*. Finally, bazedoxifene suppresses UBC6e in female islets via ERα action on a functional ERE. In contrast, bazedoxifene does not provide β cell protection in adult male Akita mice and cells. Further, unlike CE, bazedoxifene does not stabilize HRD1 and SEL1L proteins and does not mitigate ER stress in male Akita β cells. Unlike in female islets, bazedoxifene has no effect on UBC6e mRNA expression and cannot suppress the ERE-regulated Esr1 gene in male islets. Finally, in male Akita β cells transfected with an ERE reporter construct, we confirm that bazedoxifene reverses the agonistic effect of CE and E2 on ERE signaling, demonstrating that bazedoxifene is an ERα antagonist regarding ERE-mediated transcription in these cells. This is a unique example of a ligand that acts as an agonist of a nuclear receptor in females but an antagonist of the same receptor in males.

What is the mechanism of bazedoxifene sexually dimorphic activation of ERα in β cells? The ERα agonistic/antagonistic profile of a ligand in female cells depends on cell-specific features of the cellular environment (Mauvais-Jarvis et al., 2013; Nilsson et al., 2001). The activity of ERα is controlled by the binding of estrogens or SERMs to the ligand-binding domain which triggers conformational changes of ERα, receptor dimerization and binding to EREs on DNA, as well as interaction with coregulators (chromatin remodelers, coactivators, and corepressors). Each SERM induces a unique ERα conformation (Lonard and O'Malley, 2006). Therefore, the sex-dimorphic response of ERα to BZA in β cells could be driven by sex-specific cellular environments promoting recruitment of sex-specific coregulator complexes to ERα and leading to different responses in male and females (McDonnell and Wardell, 2010). Unfortunately, this cellular environment cannot be reliably studied in culture. Sex differences are dynamic and changeable properties of the body influenced by sex chromosomes and sex hormones (Mauvais-Jarvis et al., 2017a). The resultant *in vivo* male and female environments differ in multiple factors that produce different biological systems for male and female cells *in vivo* that cannot be replicated in cell culture (Mauvais-Jarvis et al., 2017a).

There are clinical ramifications to this study. First, the effect of CE to delay T2D onset in postmenopausal women could be due, at least partially, to prevention of misfolded proinsulin accumulation. The new combination of CE with bazedoxifene is an ERAD activator that opens translational potential to protect β cells in postmenopausal women. Second, several insulin gene mutations produce misfolded proinsulin and neonatal insulin-deficient diabetes in humans, including the $C^{96}Y$ Akita (Liu et al., 2010). Further studies are warranted to determine if selective estrogen ligands can promote $C^{96}Y$ proinsulin insulin degradation and prevent diabetes in humans. Third and finally, this study has far-reaching clinical implications for other conditions associated with protein misfolding (i.e., Alzheimer's disease and Parkinson disease).

EXPERIMENTAL PROCEDURES

Experimental Animals and Treatments

Male and female heterozygous Akita (C57BL/6-$Ins2^{Akita}$/J, Jackson Laboratory) mice were treated daily with oral gavage of vehicle or active compounds at the following dosage: CE (2.5 mg/kg/day) and BZA (3 mg/kg/day). Female Akita mice were subjected to ovariectomy or sham operation prior to oral treatments. Following completion of treatments, mice were euthanized, and the pancreata were immediately removed and weighed. Experiments were performed in compliance with Tulane University Institutional Animal Care and Use Committee (IACUC) and in accordance with NIH guidelines.

Metabolic Studies

Random-fed blood glucose was measured by tail bleeding. For the GTT, mice were fasted overnight for 15 hr prior to intraperitoneal (i.p.) injection of glucose (2 g/kg). Blood glucose concentrations were measured using a TRUEresult Glucose Meter (Nipro Diagnostics). Plasma insulin levels were quantified using the Rat/Mouse Insulin ELISA Kit (Millipore).

Quantification of β Cell Mass

This was performed by morphometric analysis (Tiano et al., 2011). Paraffin-embedded 5-μm-thick sections were incubated with polyclonal guinea pig anti-insulin primary antibody (1:1,000 dilution, Linco). Insulin-stained sections were visualized using Cy-3 conjugated donkey anti-guinea pig secondary antibody (Jackson Immunoresearch). Insulin-positive cells were imaged with Nikon Eclipse Ti-S epifluorescent microscope at 20× magnification. Pictures of entire pancreas sections were obtained with Aperio ScanScope slide scanner. Insulin-positive cell areas were quantified with ImageJ software. The β cell mass was calculated as pancreas weight (mg) multiplied by the percentage of insulin-positive islet area.

Quantification of β Cell Apoptosis

This was performed using TUNEL (*In Situ* Cell Death Detection Kit, TMR red, Roche Diagnosis), insulin antibody, and nuclear DAPI. The percentage of apoptotic cells was determined by dividing the number of TUNEL/insulin/DAPI-positive cells by the number of insulin-positive cells in each islet.

Transmission Electron Microscopy

Islets were fixed with 2% paraformaldehyde/2.5% glutaraldehyde/100 mM sodium cacodylate buffer at the Molecular Microbiology Imaging Facility of Washington University School of Medicine in St. Louis. β cells were imaged with transmission electron microscopy (TEM) at 10,000× magnification. We quantified mitochondrial area and ER dilation in β cells of at least 7 TEM fields using ImageJ. The ER lumen was measured at three different positions, and the mean value was calculated.

Cell Culture and Treatments

$Ins2^{+/Akita}$ cells were obtained from Dr. Koizumi Laboratory at Kyoto University and cultured in phenol red-free DMEM medium (D5921, Sigma-Aldrich), supplemented with 15% charcoal stripped-fetal bovine serum (CS-FBS)-containing vehicle (ethanol), BZA (10^{-7} M), CE (10^{-8} M), or the combination of BZA and CE. CE were prepared with the 10 components of Premarin (Pfizer) (Berrodin et al., 2009) (Table S2). After incubation with compounds for 24 hr, cells underwent ER stress induction via Tg (200 nM) for 4 hr.

Mouse Islet Isolation and Dispersion

Mouse islet isolation was performed as previously described (Tiano et al., 2011). Briefly, the common bile duct was cannulated, and the pancreas was perfused with solution of Hank's balanced salt solution (HBSS) containing collagenase (1.5 mg/mL, Sigma-Aldrich). Pancreas was excised, digested for 10 min, and rinsed with ice-cold HBSS. Islets were hand-picked under a dissection microscope and transferred into a dish filled with RPMI-1640 medium (GIBCO), supplemented with 10% CS-FBS containing compounds. The following day, islets were dispersed in individual cells using Trypsin (0.05%) and transferred into chamber slides (#154534, Thermo Scientific) with the same treatment. After 24 hr, dispersed islet cells were treated with Tg and compounds for 4 hr. Cells were fixed with 10% formalin and processed for immunostaining.

Human Islet Culture

Human islets from non-diabetic female donors were provided by the Integrated Islet Distribution Program and cultured in phenol-red-free CMRL 1066 medium (15-110-CV, Corning) supplemented with 10% CS-FBS and L-glutamine (2 mM). The next day, islets were replenished with fresh medium and treated as mouse islets.

Plasmid DNA and siRNA Transfection

Mouse Hrd1 gene open reading frame (ORF) cDNA expression plasmid and mouse Ubc6e gene ORF cDNA expression plasmid was purchased from Origene (pCMV6-Hrd1 and pCMV6-Ubc6e). Insulin-2-HA-pcDNA3, insulin-2 C96Y-HA-pcDNA3, and Flag Ub WT plasmid were obtained as described (Allen et al., 2004). hERα/pcDNA3.1 plasmid was provided by Brian Rowan from Tulane University. Plasmids were purified with QIAGEN Plasmid Maxi Kit (QIAGEN). For SEL1L knockdown experiments, small interfering RNAs (siRNAs) specific for mouse SEL1L (Silencer Select Pre-Designed siRNA) and a non-targeting negative control siRNA (Silencer Select Negative Control) were purchased from Thermo Fisher Scientific. Transient transfections of plasmid DNA were performed using Lipofectamine 2000 reagent (Thermo Fisher Scientific). Transfections of siRNAs were performed with Lipofectamine RNAiMAX Transfection Reagent (Thermo Fisher Scientific).

Protein Stability Assay

Ins2$^{+/Akita}$ cells cultured in phenol red-free DMEM medium supplemented with 15% charcoal-stripped fetal bovine serum (CS-FBS) containing compounds for 24 hr. Cells were treated with Tg and compounds for 1 hr, followed by treatment with cycloheximide (CHX, 100 μg/mL, Sigma-Aldrich), and harvested at the indicated time points. The proteasome inhibitor MG132 (10 μM, Sigma-Aldrich) was added along with CHX when necessary. Cell lysates were subjected to western blotting.

Western Blot

Protein extracts from cells or islets were obtained using M-PER Mammalian Protein Extraction Reagent (Thermo Fisher Scientific) supplemented with protease inhibitor (Roche Applied Science). Protein lysates were resolved by SDS-PAGE. The following primary antibodies were used for immunoblotting: CHOP (2895, Cell Signaling), HRD1 (sc-130889, Santa Cruz), SEL1L (ab78298, Abcam), UBC6e (sc-292491, Santa Cruz), Actin (sc-1616, Santa Cruz) and α-Tubulin (MS-581-P0, Neomarkers). Western blots were developed with enhanced chemiluminescence (Supersignal West Pico Chemiluminescent Substrate, Thermo Fisher Scientific). The band intensities were quantified using ImageJ.

qRT-PCR

Total RNA from was extracted using the RNeasy Plus Mini Kit (QIAGEN) and reverse transcribed into cDNA using an iScript cDNA Synthesis kit (Bio-Rad). qPCR was performed using iTaq Universal SYBR Green Supermix (Bio-Rad) and the iCycler iQ Real-Time PCR Detection System (Bio-Rad). β-actin was used as the housekeeping gene.

Transient Transfection of COS-7 Cells and Analysis of Proinsulin Ubiquitination and Stability

COS-7 cells were placed in CS-DMEM and high-glucose medium with 10% CS-FBS. Transient transfections were carried out using 1.5 μg cDNA/well and Polyfect (QIAGEN). The cells were transfected with hemagglutinin A (HA)-WT proinsulin or HA-C^{96}Y proinsulin along with ERα and FLAG-ubiquitin in the absence or in the presence of HRD-1 (0.375 μg/plasmid). Cells were treated with compounds starting 24 hr after transfection, and, at 48 hr, Tg (20 nM) was added for 4 hr. Whole-cell protein lysates were resolved by SDS-PAGE, and western blotting was performed using antibodies against a HA epitope tag (BioLegend #901513 at 1:2,000) or a Flag epitope tag (Sigma, #F1804, 1:500). The results were visualized with horseradish peroxidase (HRP)-conjugated secondary antibodies (Jackson ImmunoResearch) and enhanced chemiluminescence (Thermo Fisher-Pierce). Immunoprecipitation of cell extracts was carried out with 300 μg total protein using protein A/B plus agarose (Pierce, Thermo Scientific) and mouse-anti-HA epitope antibody (1:100 dilution). The immunoprecipitates were subjected to gel electrophoresis and immunoblotting with anti-FLAG antibody.

ERE-Luc Transfection and Luciferase Assay

ERE-Luc transfection and a luciferase assay were performed following Wong et al. (2010). MIN6 cells were cultured in phenol-red-free DMEM and transfected with 0.8 μg of ERE-Luc using 2 μL of Lipofectamine 2000. After 6-hr incubation, cells were then treated with compounds (E_2: 10^{-8} M) for 24 hr. Measurement of ERE luciferase activity was performed using a Luciferase Assay System (Promega). Values are reported as relative luciferase units corrected for protein concentration.

Statistics

Results were presented as means ± SEM and analyzed by Student's t test or one-way ANOVA, followed by the Bonferroni test when appropriate using the Graphpad Prism (v.5) software. $p < 0.05$ is considered statistically significant.

SUPPLEMENTAL INFORMATION

Supplemental Information includes Supplemental Experimental Procedures, five figures, and two tables and can be found with this article online at https://doi.org/10.1016/j.celrep.2018.06.019.

ACKNOWLEDGMENTS

This work was supported by grants from the NIH (DK074970 and DK107444), by a Department of Veterans Affairs Merit Review Award (BX003725), and by an investigator-initiated award from Pfizer (WS2069876) to F.M.-J. and, in part, by a LA CaTS Center grant (1 U54 GM104940). Z.E.F. was supported by an NIH grant (DK099625). P.A. was supported by NIH grant (DK48280), and K.S.K. was supported by the Division of Intramural Research, NIEHS/NIH (1ZIAES70065).

AUTHOR CONTRIBUTIONS

F.M.-J. conceived of the idea, designed the experiments, analyzed the data, and wrote and edited the manuscript. B.X. designed and performed the experiments, analyzed the data, and wrote the manuscript. C.A., A.I.A.-M., T.F., and J.H.K. performed the experiments. L.A.C. provided the locations of EREs on the chromosome that contains the Ube2j1 gene in the mouse and human genomes. S.C.H. and K.S.K. generated and provided ERαKO and ERβKO mice. E.R.L. generated and provided MOER and NOER mice. P.A. participated in the design and interpretation of the experiments of proinsulin turnover and edited the manuscript. F.U. provided HRD1, ubiquitin, and WT and mutant proinsulin plasmids. Z.E.F. participated in the design and interpretation of the experiments of HRD1 and SEL1L protein turnover, performed experiments of proinsulin ubiquitination, and edited the manuscript.

DECLARATION OF INTERESTS

F.M.J. was a scientific advisory board member and received an investigator-initiated research grant from Pfizer, Inc. All other authors declare no competing interests.

Received: January 9, 2018
Revised: May 11, 2018
Accepted: June 1, 2018
Published: July 3, 2018

REFERENCES

Allen, J.R., Nguyen, L.X., Sargent, K.E., Lipson, K.L., Hackett, A., and Urano, F. (2004). High ER stress in beta-cells stimulates intracellular degradation of misfolded insulin. Biochem. Biophys. Res. Commun. *324*, 166–170.

Back, S.H., and Kaufman, R.J. (2012). Endoplasmic reticulum stress and type 2 diabetes. Annu. Rev. Biochem. *81*, 767–793.

Berrodin, T.J., Chang, K.C., Komm, B.S., Freedman, L.P., and Nagpal, S. (2009). Differential biochemical and cellular actions of Premarin estrogens: distinct pharmacology of bazedoxifene-conjugated estrogens combination. Mol. Endocrinol. *23*, 74–85.

Burr, M.L., Cano, F., Svobodova, S., Boyle, L.H., Boname, J.M., and Lehner, P.J. (2011). HRD1 and UBE2J1 target misfolded MHC class I heavy chains for endoplasmic reticulum-associated degradation. Proc. Natl. Acad. Sci. USA *108*, 2034–2039.

Chambliss, K.L., Wu, Q., Oltmann, S., Konaniah, E.S., Umetani, M., Korach, K.S., Thomas, G.D., Mineo, C., Yuhanna, I.S., Kim, S.H., et al. (2010). Non-nuclear estrogen receptor alpha signaling promotes cardiovascular protection but not uterine or breast cancer growth in mice. J. Clin. Invest. *120*, 2319–2330.

Coons, L.A., Hewitt, S.C., Burkholder, A.B., McDonnell, D.P., and Korach, K.S. (2017). DNA sequence constraints define functionally active steroid nuclear receptor binding sites in chromatin. Endocrinology *158*, 3212–3234.

Dauvois, S., Danielian, P.S., White, R., and Parker, M.G. (1992). Antiestrogen ICI 164,384 reduces cellular estrogen receptor content by increasing its turnover. Proc. Natl. Acad. Sci. USA *89*, 4037–4041.

Eizirik, D.L., and Cnop, M. (2010). ER stress in pancreatic beta cells: the thin red line between adaptation and failure. Sci. Signal. *3*, pe7.

Espeland, M.A., Hogan, P.E., Fineberg, S.E., Howard, G., Schrott, H., Waclawiw, M.A., and Bush, T.L. (1998). Effect of postmenopausal hormone therapy

on glucose and insulin concentrations. PEPI Investigators. Postmenopausal Estrogen/Progestin Interventions. Diabetes Care *21*, 1589–1595.

Haataja, L., Manickam, N., Soliman, A., Tsai, B., Liu, M., and Arvan, P. (2016). Disulfide mispairing during proinsulin folding in the endoplasmic reticulum. Diabetes *65*, 1050–1060.

Hagiwara, M., Ling, J., Koenig, P.A., and Ploegh, H.L. (2016). Posttranscriptional regulation of glycoprotein quality control in the endoplasmic reticulum is controlled by the E2 Ub-conjugating enzyme UBC6e. Mol. Cell *63*, 753–767.

Harrington, W.R., Kim, S.H., Funk, C.C., Madak-Erdogan, Z., Schiff, R., Katzenellenbogen, J.A., and Katzenellenbogen, B.S. (2006). Estrogen dendrimer conjugates that preferentially activate extranuclear, nongenomic versus genomic pathways of estrogen action. Mol. Endocrinol. *20*, 491–502.

He, K., Cunningham, C.N., Manickam, N., Liu, M., Arvan, P., and Tsai, B. (2015). PDI reductase acts on Akita mutant proinsulin to initiate retrotranslocation along the Hrd1/Sel1L-p97 axis. Mol. Biol. Cell *26*, 3413–3423.

Hewitt, S.C., Li, L., Grimm, S.A., Winuthayanon, W., Hamilton, K.J., Pockette, B., Rubel, C.A., Pedersen, L.C., Fargo, D., Lanz, R.B., et al. (2014). Novel DNA motif binding activity observed in vivo with an estrogen receptor α mutant mouse. Mol. Endocrinol. *28*, 899–911.

Iida, Y., Fujimori, T., Okawa, K., Nagata, K., Wada, I., and Hosokawa, N. (2011). SEL1L protein critically determines the stability of the HRD1-SEL1L endoplasmic reticulum-associated degradation (ERAD) complex to optimize the degradation kinetics of ERAD substrates. J. Biol. Chem. *286*, 16929–16939.

Kanaya, A.M., Herrington, D., Vittinghoff, E., Lin, F., Grady, D., Bittner, V., Cauley, J.A., and Barrett-Connor, E.; Heart and Estrogen/progestin Replacement Study (2003). Glycemic effects of postmenopausal hormone therapy: the Heart and Estrogen/progestin Replacement Study. A randomized, double-blind, placebo-controlled trial. Ann. Intern. Med. *138*, 1–9.

Kaneko, M., Koike, H., Saito, R., Kitamura, Y., Okuma, Y., and Nomura, Y. (2010). Loss of HRD1-mediated protein degradation causes amyloid precursor protein accumulation and amyloid-beta generation. J. Neurosci. *30*, 3924–3932.

Kharode, Y., Bodine, P.V., Miller, C.P., Lyttle, C.R., and Komm, B.S. (2008). The pairing of a selective estrogen receptor modulator, bazedoxifene, with conjugated estrogens as a new paradigm for the treatment of menopausal symptoms and osteoporosis prevention. Endocrinology *149*, 6084–6091.

Kilic, G., Alvarez-Mercado, A.I., Zarrouki, B., Opland, D., Liew, C.W., Alonso, L.C., Myers, M.G., Jr., Jonas, J.C., Poitout, V., Kulkarni, R.N., and Mauvais-Jarvis, F. (2014). The islet estrogen receptor-α is induced by hyperglycemia and protects against oxidative stress-induced insulin-deficient diabetes. PLoS ONE *9*, e87941.

Komm, B.S. (2008). A new approach to menopausal therapy: the tissue selective estrogen complex. Reprod. Sci. *15*, 984–992.

Komm, B.S., Vlasseros, F., Samadfam, R., Chouinard, L., and Smith, S.Y. (2011). Skeletal effects of bazedoxifene paired with conjugated estrogens in ovariectomized rats. Bone *49*, 376–386.

Le May, C., Chu, K., Hu, M., Ortega, C.S., Simpson, E.R., Korach, K.S., Tsai, M.J., and Mauvais-Jarvis, F. (2006). Estrogens protect pancreatic beta-cells from apoptosis and prevent insulin-deficient diabetes mellitus in mice. Proc. Natl. Acad. Sci. USA *103*, 9232–9237.

Lindsay, R., Gallagher, J.C., Kagan, R., Pickar, J.H., and Constantine, G. (2009). Efficacy of tissue-selective estrogen complex of bazedoxifene/conjugated estrogens for osteoporosis prevention in at-risk postmenopausal women. Fertil. Steril. *92*, 1045–1052.

Liu, S., and Mauvais-Jarvis, F. (2009). Rapid, nongenomic estrogen actions protect pancreatic islet survival. Islets *1*, 273–275.

Liu, S., Le May, C., Wong, W.P., Ward, R.D., Clegg, D.J., Marcelli, M., Korach, K.S., and Mauvais-Jarvis, F. (2009). Importance of extranuclear estrogen receptor-alpha and membrane G protein-coupled estrogen receptor in pancreatic islet survival. Diabetes *58*, 2292–2302.

Liu, M., Hodish, I., Haataja, L., Lara-Lemus, R., Rajpal, G., Wright, J., and Arvan, P. (2010). Proinsulin misfolding and diabetes: mutant INS gene-induced diabetes of youth. Trends Endocrinol. Metab. *21*, 652–659.

Liu, S., Kilic, G., Meyers, M.S., Navarro, G., Wang, Y., Oberholzer, J., and Mauvais-Jarvis, F. (2013). Oestrogens improve human pancreatic islet transplantation in a mouse model of insulin deficient diabetes. Diabetologia *56*, 370–381.

Lonard, D.M., and O'Malley, B.W. (2006). The expanding cosmos of nuclear receptor coactivators. Cell *125*, 411–414.

Manson, J.E., and Kaunitz, A.M. (2016). Menopause management–getting clinical care back on track. N. Engl. J. Med. *374*, 803–806.

Manson, J.E., Chlebowski, R.T., Stefanick, M.L., Aragaki, A.K., Rossouw, J.E., Prentice, R.L., Anderson, G., Howard, B.V., Thomson, C.A., LaCroix, A.Z., et al. (2013). Menopausal hormone therapy and health outcomes during the intervention and extended poststopping phases of the Women's Health Initiative randomized trials. JAMA *310*, 1353–1368.

Margolis, K.L., Bonds, D.E., Rodabough, R.J., Tinker, L., Phillips, L.S., Allen, C., Bassford, T., Burke, G., Torrens, J., and Howard, B.V.; Women's Health Initiative Investigators (2004). Effect of oestrogen plus progestin on the incidence of diabetes in postmenopausal women: results from the Women's Health Initiative Hormone Trial. Diabetologia *47*, 1175–1187.

Mauvais-Jarvis, F., Clegg, D.J., and Hevener, A.L. (2013). The role of estrogens in control of energy balance and glucose homeostasis. Endocr. Rev. *34*, 309–338.

Mauvais-Jarvis, F., Arnold, A.P., and Reue, K. (2017a). A guide for the design of pre-clinical studies on sex differences in metabolism. Cell Metab. *25*, 1216–1230.

Mauvais-Jarvis, F., Manson, J.E., Stevenson, J.C., and Fonseca, V.A. (2017b). Menopausal hormone therapy and type 2 diabetes prevention: evidence, mechanisms, and clinical implications. Endocr. Rev. *38*, 173–188.

McDonnell, D.P., and Wardell, S.E. (2010). The molecular mechanisms underlying the pharmacological actions of ER modulators: implications for new drug discovery in breast cancer. Curr. Opin. Pharmacol. *10*, 620–628.

Nilsson, S., Mäkelä, S., Treuter, E., Tujague, M., Thomsen, J., Andersson, G., Enmark, E., Pettersson, K., Warner, M., and Gustafsson, J.A. (2001). Mechanisms of estrogen action. Physiol. Rev. *81*, 1535–1565.

Noack, J., Bernasconi, R., and Molinari, M. (2014). How viruses hijack the ERAD tuning machinery. J. Virol. *88*, 10272–10275.

Oyadomari, S., and Mori, M. (2004). Roles of CHOP/GADD153 in endoplasmic reticulum stress. Cell Death Differ. *11*, 381–389.

Papa, F.R. (2012). Endoplasmic reticulum stress, pancreatic β-cell degeneration, and diabetes. Cold Spring Harb. Perspect. Med. *2*, a007666.

Pedram, A., Razandi, M., Kim, J.K., O'Mahony, F., Lee, E.Y., Luderer, U., and Levin, E.R. (2009). Developmental phenotype of a membrane only estrogen receptor alpha (MOER) mouse. J. Biol. Chem. *284*, 3488–3495.

Pedram, A., Razandi, M., Lewis, M., Hammes, S., and Levin, E.R. (2014). Membrane-localized estrogen receptor α is required for normal organ development and function. Dev. Cell *29*, 482–490.

Pedram, A., Razandi, M., Blumberg, B., and Levin, E.R. (2015). Membrane and nuclear estrogen receptor α collaborate to suppress adipogenesis but not triglyceride content. FASEB J. *30*, 230–240.

Qi, L., Tsai, B., and Arvan, P. (2017). New insights into the physiological role of endoplasmic reticulum-associated degradation. Trends Cell Biol. *27*, 430–440.

Rogers, T.B., Inesi, G., Wade, R., and Lederer, W.J. (1995). Use of thapsigargin to study Ca2+ homeostasis in cardiac cells. Biosci. Rep. *15*, 341–349.

Salpeter, S.R., Walsh, J.M., Ormiston, T.M., Greyber, E., Buckley, N.S., and Salpeter, E.E. (2006). Meta-analysis: effect of hormone-replacement therapy on components of the metabolic syndrome in postmenopausal women. Diabetes Obes. Metab. *8*, 538–554.

Santen, R.J., Allred, D.C., Ardoin, S.P., Archer, D.F., Boyd, N., Braunstein, G.D., Burger, H.G., Colditz, G.A., Davis, S.R., Gambacciani, M., et al.; Endocrine Society (2010). Postmenopausal hormone therapy: an Endocrine Society scientific statement. J. Clin. Endocrinol. Metab. *95* (*7, Suppl 1*), s1–s66.

Smith, M.H., Ploegh, H.L., and Weissman, J.S. (2011). Road to ruin: targeting proteins for degradation in the endoplasmic reticulum. Science *334*, 1086–1090.

Taylor, R.C. (2016). Aging and the UPR(ER). Brain Res. *1648* (*Pt B*), 588–593.

Tiano, J.P., and Mauvais-Jarvis, F. (2012). Importance of oestrogen receptors to preserve functional β-cell mass in diabetes. Nat. Rev. Endocrinol. *8*, 342–351.

Tiano, J.P., Delghingaro-Augusto, V., Le May, C., Liu, S., Kaw, M.K., Khuder, S.S., Latour, M.G., Bhatt, S.A., Korach, K.S., Najjar, S.M., et al. (2011). Estrogen receptor activation reduces lipid synthesis in pancreatic islets and prevents β cell failure in rodent models of type 2 diabetes. J. Clin. Invest. *121*, 3331–3342.

Tiano, J.P., Tate, C.R., Yang, B.S., DiMarchi, R., and Mauvais-Jarvis, F. (2015). Effect of targeted estrogen delivery using glucagon-like peptide-1 on insulin secretion, insulin sensitivity and glucose homeostasis. Sci. Rep. *5*, 10211.

Tsutsumi, S., Gotoh, T., Tomisato, W., Mima, S., Hoshino, T., Hwang, H.J., Takenaka, H., Tsuchiya, T., Mori, M., and Mizushima, T. (2004). Endoplasmic reticulum stress response is involved in nonsteroidal anti-inflammatory drug-induced apoptosis. Cell Death Differ. *11*, 1009–1016.

Wang, M., and Kaufman, R.J. (2016). Protein misfolding in the endoplasmic reticulum as a conduit to human disease. Nature *529*, 326–335.

Wardell, S.E., Nelson, E.R., Chao, C.A., and McDonnell, D.P. (2013). Bazedoxifene exhibits antiestrogenic activity in animal models of tamoxifen-resistant breast cancer: implications for treatment of advanced disease. Clin. Cancer Res. *19*, 2420–2431.

Wijayaratne, A.L., and McDonnell, D.P. (2001). The human estrogen receptor-alpha is a ubiquitinated protein whose stability is affected differentially by agonists, antagonists, and selective estrogen receptor modulators. J. Biol. Chem. *276*, 35684–35692.

Wong, W.P., Tiano, J.P., Liu, S., Hewitt, S.C., Le May, C., Dalle, S., Katzenellenbogen, J.A., Katzenellenbogen, B.S., Korach, K.S., and Mauvais-Jarvis, F. (2010). Extranuclear estrogen receptor-alpha stimulates NeuroD1 binding to the insulin promoter and favors insulin synthesis. Proc. Natl. Acad. Sci. USA *107*, 13057–13062.

Zhou, S., Zhao, L., Yi, T., Wei, Y., and Zhao, X. (2016). Menopause-induced uterine epithelium atrophy results from arachidonic acid/prostaglandin E2 axis inhibition-mediated autophagic cell death. Sci. Rep. *6*, 31408.

Cell Reports, Volume *24*

Supplemental Information

Estrogens Promote Misfolded Proinsulin Degradation to Protect Insulin Production and Delay Diabetes

Beibei Xu, Camille Allard, Ana I. Alvarez-Mercado, Taylor Fuselier, Jun Ho Kim, Laurel A. Coons, Sylvia C. Hewitt, Fumihiko Urano, Kenneth S. Korach, Ellis R. Levin, Peter Arvan, Z. Elizabeth Floyd, and Franck Mauvais-Jarvis

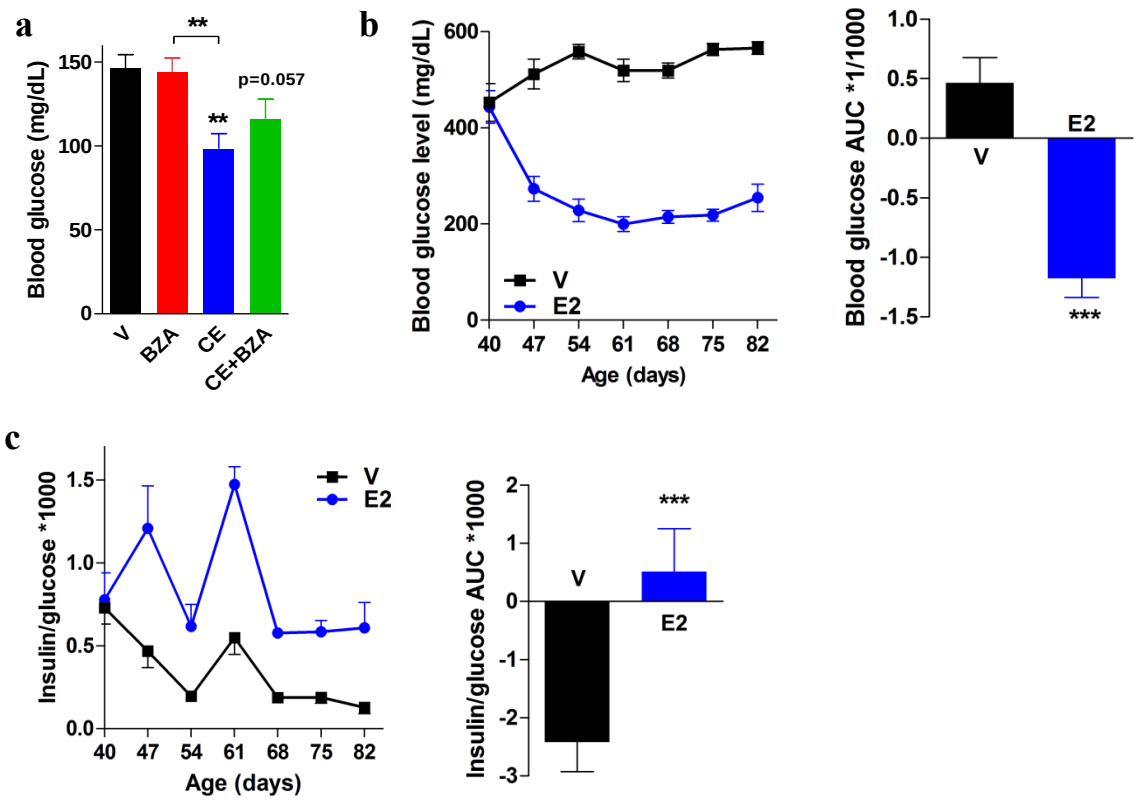

Figure S1. Related to Figure 1. (**a**) Overnight fasting blood glucose levels in 8-week-old male Akita mice (from Fig.1) treated as indicated. Data are shown as mean ± SEM. **P < 0.01. (**b**) Random fed blood glucose concentrations and corresponding blood glucose AUC in male Akita mice of the indicated age receiving E_2 treatment starting at 40 days of age. (**c**) Plasma insulin/blood glucose ratio and corresponding AUC in the same groups of mice as in Figure S1b (n=8). Data are shown as mean ± SEM. ***P < 0.001.

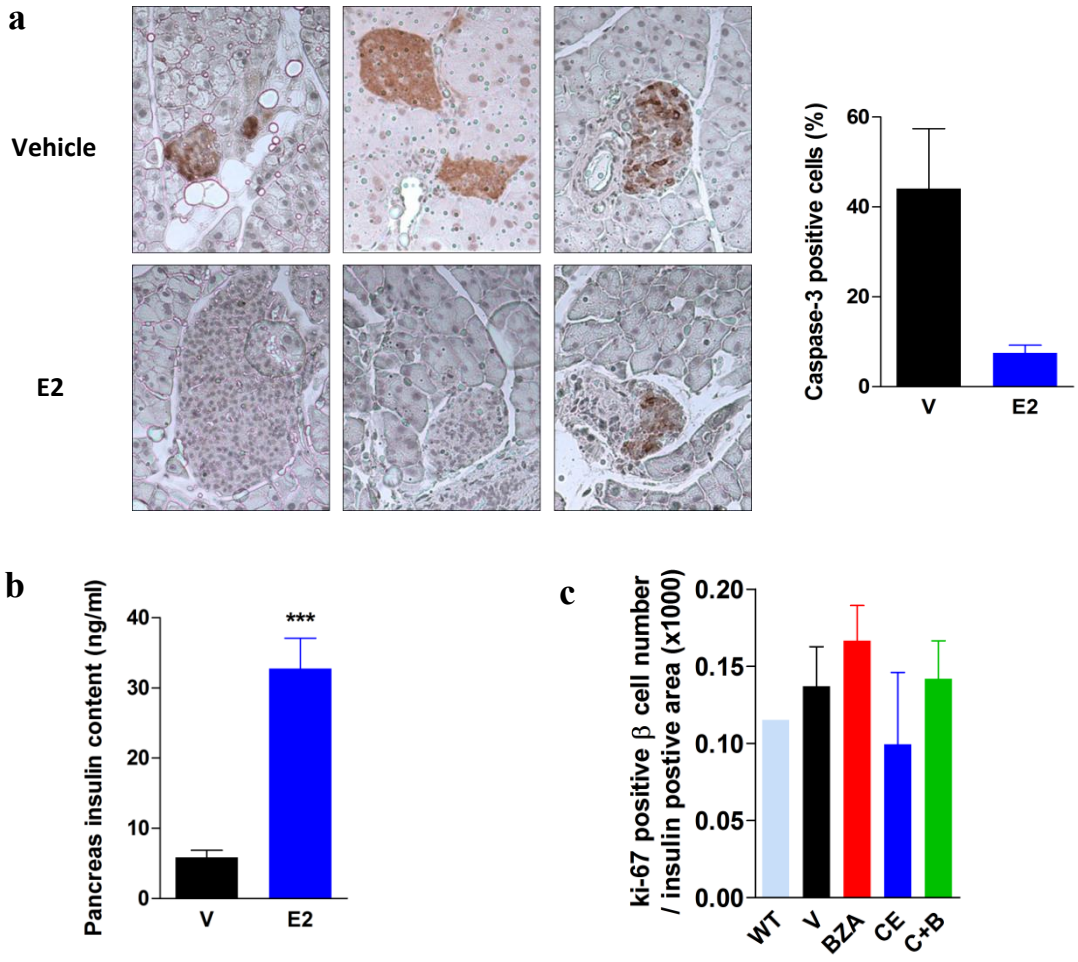

Figure S2. Related to Figure 2. (**a**) Representative images for Caspase-3 staining in pancreatic islets from male Akita mice from Figure S1b and quantification of Caspase-3 positive cell in the same groups of islets (n=3 experiments). (**b**) Pancreatic insulin content in male Akita mice from Figure S1b (n=5-8). (**c**) Quantification of pancreatic β-cell proliferation in male Akita mice from Fig. 2f was quantified by ki-67 staining (n = 3). Data are shown as mean ± SEM. *P < 0.05, **P < 0.01, ***P < 0.001.

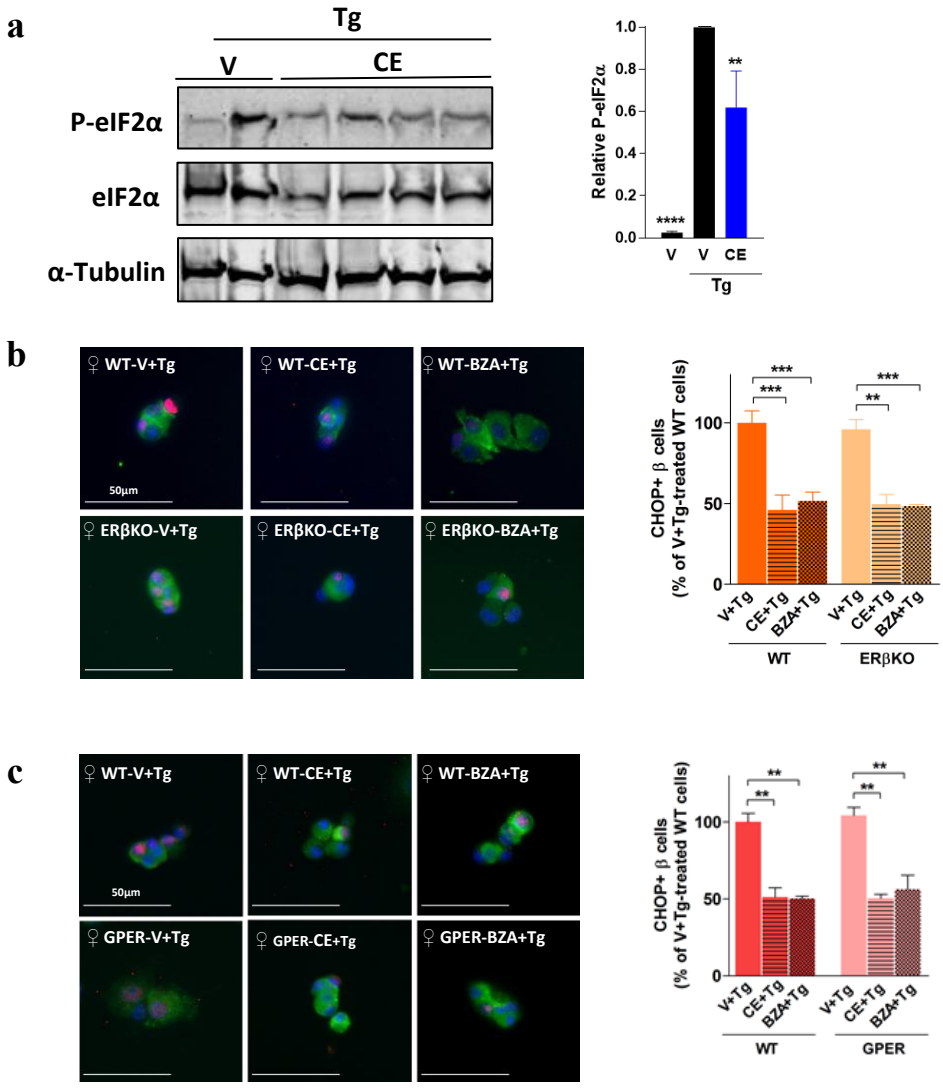

Figure S3. Related to Figure 3. (**a**) Male Ins2$^{+/Akita}$ β-cells were treated with the indicated compounds for 24h followed by exposure to Tg for 4h. Representative Western blot for elf2α protein phosphorylation and total protein (left) and relative elf2α phosphorylation/total protein levels quantified by densitometry (right) are shown (n=4 experiments). (**b**) Dispersed islets from female WT, ERβKO and (**c**) GPERKO mice were treated with the indicated compounds for 24h followed by exposure to Tg for 4h. Representative images of immunofluorescent staining for CHOP (red), insulin (green) and nuclei (blue) and quantification of β-cells with CHOP^{+} nuclei relative to vehicle are shown (n=3 experiments). Data are shown as mean ± SEM. **P < 0.01, ***P < 0.001.

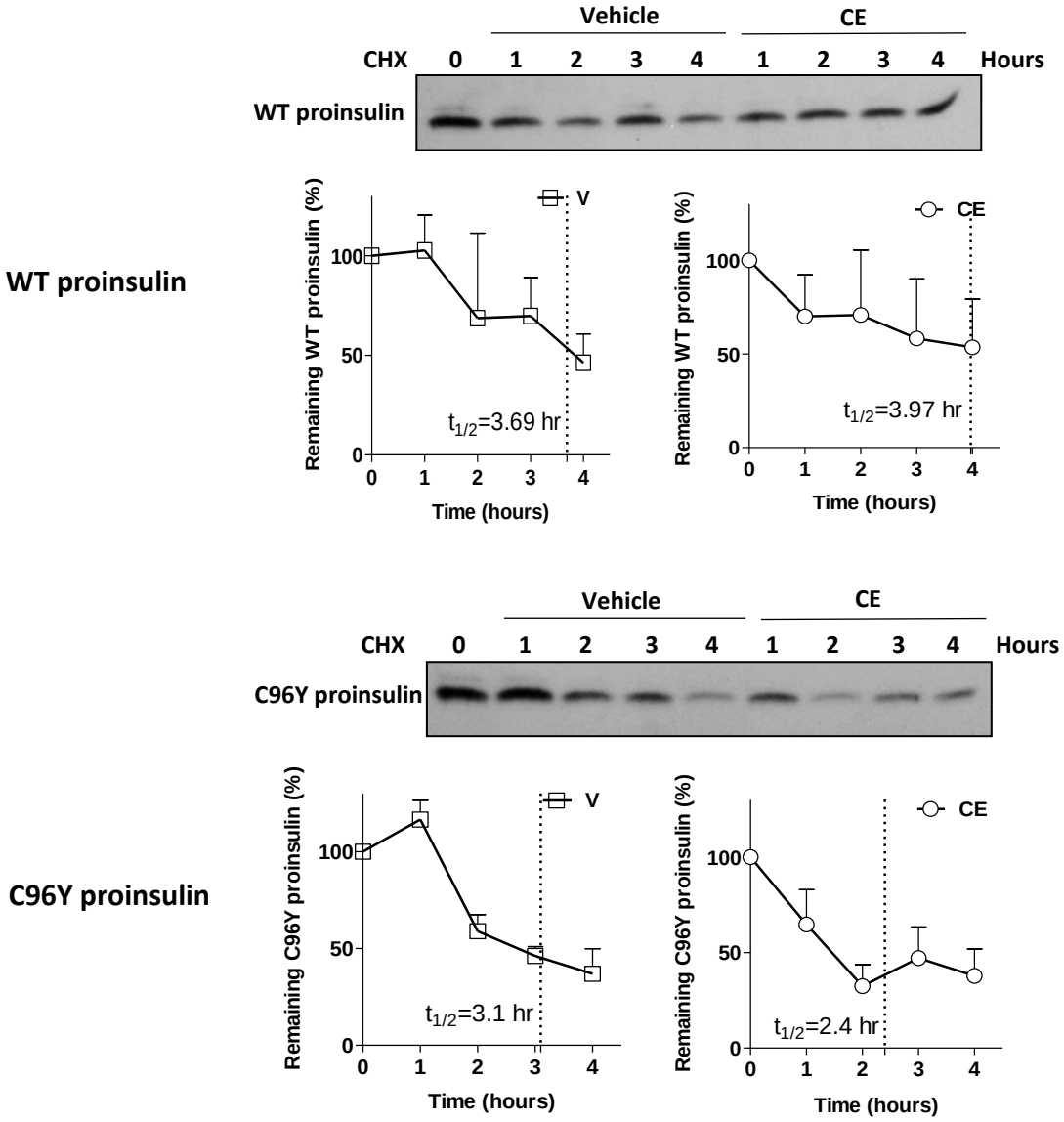

Figure S4. Related to Figure 4. COS-7 cells were transfected with HA-wild-type proinsulin or HA-C96Y proinsulin along with ERα and HRD1. 48h after transfection, cells were treated with CE (10 nM) or vehicle (V) along with 100 mM cycloheximide (CHX) and cell lysates were harvested each hour for four hours. A zero time point sample was obtained prior to treating the cells with CHX -/+ CE. Western blotting was carried out using anti-HA antibodies. Quantification by densitometry of decay curves for WT and C96Y proinsulin following V or CE treatments are shown. Inserts represent the half-life of proinsulin for each condition ($t_{1/2}$) (n=3 distinct experiments/condition).

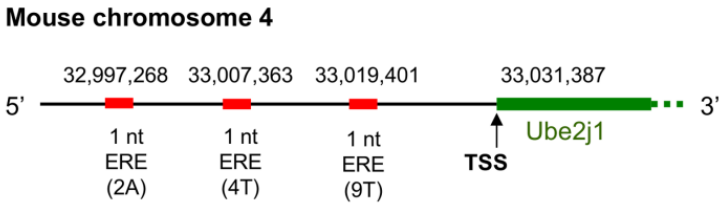

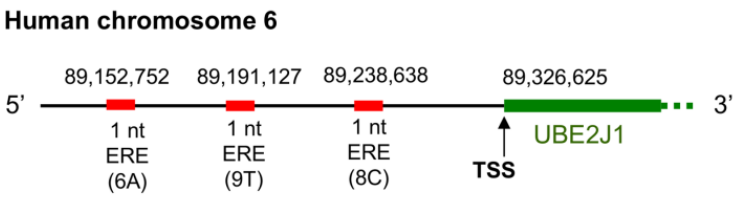

perfect ERE and 1 nt variant EREs in front of UBE2J1 on chromosome 4 for mouse			
chromosome number	**Start location of motif on chromosome**	**End location of motif on chromosome**	**ERE type**
chr4	32,661,599	32,661,612	ERE
chr4	32,690,300	32,690,313	1T
chr4	32,724,603	32,724,616	9T
chr4	32,774,406	32,774,419	8C
chr4	32,788,091	32,788,104	9T
chr4	32,853,256	32,853,269	2C
chr4	32,879,113	32,879,126	5T
chr4	32,926,038	32,926,051	3C
chr4	32,978,635	32,978,648	9T
chr4	32,978,743	32,978,756	9A
chr4	32,980,093	32,980,106	7A
chr4	32,997,268	32,997,281	2A
chr4	33,007,363	33,007,376	4T
chr4	33,019,401	33,019,414	9T

perfect ERE and 1 nt variant EREs in front of UBE2J1 on chromosome 6 for human			
chromosome number	**Start location of motif on chromosome**	**End location of motif on chromosome**	**ERE type**
chr6	88,835,722	88,835,735	ERE
chr6	88,878,623	88,878,636	3C
chr6	88,917,482	88,917,495	7C
chr6	88,921,213	88,921,226	5C
chr6	88,975,485	88,975,498	3C
chr6	88,981,733	88,981,746	3C
chr6	89,005,445	89,005,458	5T
chr6	89,112,597	89,112,610	9A
chr6	89,123,674	89,123,687	5T
chr6	89,152,752	89,152,765	6A
chr6	89,191,127	89,191,140	9T
chr6	89,238,638	89,238,651	8C

Figure S5. Related to Figure 6. Position of perfect EREs and 1nt variant EREs in front of *Ube2j1* in the mouse (left) and human (right) genomes.

SUPPLEMENTAL EXPERIMENTAL PROCEDURES

Quantification of pancreatic β-cell proliferation. Ki-67 staining and insulin staining were performed in pancreas sections to identify β-cell proliferation. The pancreas sections were incubated with monoclonal rabbit anti-Ki-67 antibody (1:200 dilution, Thermo Scientific) and polyclonal guinea pig anti-insulin primary antibody (1: 1000 dilution, Linco, St Louis, MO). Ki-67 staining and insulin staining were visualized using Cy-3 conjugated donkey anti-rabbit secondary antibody (Jackson Immunoresearch) and FITC conjugated donkey anti-guinea pig secondary antibody (Jackson Immunoresearch), respectively. All the islets in one pancreas were imaged with Nikon Eclipse Ti-S epifluorescent microscope at 20x magnification. Insulin staining positive area in each islet was measured with ImageJ software. β-cell proliferation was determined by dividing the number of Ki-67/insulin double-positive cells by insulin staining positive area (μm^2) in each pancreas section.

Caspase-3 Immunohistochemistry Staining. 3, 3-Diaminobenzidine (DAB) (Vector Laboratories) immunohistochemical staining complex technique was performed. Briefly, deparaffinized pancreatic sections of 5μm thickness were rehydrated in ethanol and induced and antigen retrieval procedure using 0.01M Sodium Citrate Buffer (pH 6.0). Peroxidase activity was blocked with a solution of 3% hydrogen peroxide and nonspecific antibody reactions were blocked with a solution of 1% BSA, 5% goat serum, 0.02% Triton X-100. Sections were incubated overnight at 4°C with primary antibody anti-cleaved caspase 3 (Cell Signaling) and 1 hour at room temperature with secondary biotinylated anti-rabbit antibody. Sections were placed in an avidin-biotinhorseradish peroxidase (HRP) complex (ABC Elite; Vector Laboratories) for 1 hour. After rinsing sections were stained with DAB until medium-dark brown color was achieved. Finally a nuclear hematoxylin counterstain and dehydration was performed.

ERα western blot. Protein extracts from $Ins2^{+/Akita}$ cells, MCF-7 cells or Min-6 cells were obtained using M-PER Mammalian Protein Extraction Reagent (Thermo Fisher Scientific) supplemented with protease inhibitor (Roche Applied Science) following the manufacturer's protocol. Protein lysates were resolved by SDS-PAGE. The following primary antibodies were used for immunoblotting: ERα (sc-542, Santa Cruz), Actin (sc-1616, Santa Cruz). Western blots were developed with enhanced chemiluminescence (Supersignal West Pico Chemiluminescent Substrate, Thermo Fisher Scientific). The band intensities were quantified using ImageJ software.

Identification of Estrogen Response Element (ERE)s in the mouse and human genomes. The location coordinates of the perfect and 1 nt variant EREs were identified in the mouse and human genomes using OligoMatch (UCSC) as described in Coons et al. [1] Here, the ERE is the motif 5'-GGTCAnnnTGACC-3'.

SUPPLEMENTAL REFERENCES

1. Coons, L.A., Hewitt, S.C., Burkholder, A.B., McDonnell, D.P. & Korach, K.S. DNA Sequence Constraints Define Functionally Active Steroid Nuclear Receptor Binding Sites in Chromatin. *Endocrinology* 158, 3212-3234 (2017).

Table S1, related to Experimental Procedures: the characteristics of the female islet donors

	Donor #1	**Donor #2**	**Donor #3**
Age	49 Years	27 Years	65 Years
Gender	Female	Female	Female
Height	67.00 inches	61.00 inches	69.00 inches
Weight	161.0 lbs	147.0 lbs	238.0 lbs
BMI	25.2	27.8	35.1
Ethnicity/Race	Black or African American	Hispanic/Latino	Black or African American
ABO blood group	O	B	O
Cause of death	Cerebrovascular/stroke	Anoxia	Cerebrovascular/stroke
Medical history	Clean	Clean	HTN >10 yrs compliant, HLD >10 yrs

Table S2, related to Experimental Procedures: Composition of conjugated equine estrogens (CE)

Estrogens	Percentage ratio
Estrone	48%
Equilin	24%
17α-Dihydroequilin	15%
delta-8,9-Dehydroestrone	4.3%
17α-Estradiol	3.8%
17β-Dihydroequilin	1.8%
Equilenin	1.1%
17β-Estradiol	0.68%
17α-Dihydroequilenin	0.45%
17β-Dihydroequilenin	0.3%